IEEE Access
Multidisciplinary | Rapid Review | Open Access Journal

Received June 18, 2020, accepted June 25, 2020, date of publication July 3, 2020, date of current version July 15, 2020.

Digital Object Identifier 10.1109/ACCESS.2020.3007115

Comparison of IEEE 802.11p and LTE-V2X: An Evaluation With Periodic and Aperiodic Messages of Constant and Variable Size

RAFAEL MOLINA-MASEGOSA, JAVIER GOZALVEZ, (Senior Member, IEEE), AND MIGUEL SEPULCRE, (Senior Member, IEEE)
Departamento de Ingenieria de Comunicaciones, Universidad Miguel Hernández de Elche (UMH), 03202 Elche, Spain

Corresponding author: Javier Gozalvez (j.gozalvez@umh.es)

This work was supported in part by the Spanish Ministry of Science and Innovation (MCI), in part by the State Research Agency (AEI), in part by the European Regional Development Fund (FEDER) under Project TEC2017-88612-R, and in part by the Universidad Miguel Hernández de Elche (UMH) through Ayudas para la Formacion de Personal Investigador.

ABSTRACT V2X (Vehicle to everything) communications can be currently supported by standards based on IEEE 802.11p (e.g. DSRC or ITS-G5) or LTE-V2X (also known as Cellular V2X or C-V2X) technologies. There has been an intense debate in the community on which technology achieves best performance. However, existing studies do not take into account the variability present in the generation and size of V2X messages. This variability can significantly impact the operation and performance of the Medium Access Control (MAC). This study progresses the state of the art by conducting an in-depth evaluation of both technologies under different message traffic patterns. In particular, we consider aperiodic and periodic messages of constant or variable size based on the standardized ETSI Cooperative Awareness Messages (CAMs). This study considers different scenarios and possible configurations of IEEE 802.11p and LTE-V2X. We demonstrate that IEEE 802.11p can better cope with variations in the size and time interval between messages. We also demonstrate (and characterize) that the LTE-V2X sensing-based semi-persistent scheduling faces certain inefficiencies when transmitting aperiodic messages of variable size. These inefficiencies result in that IEEE 802.11p generally outperforms LTE-V2X when transmitting aperiodic messages of variable size except when the channel load is very low.

INDEX TERMS LTE-V2X, C-V2X, cellular V2X, IEEE 802.11p, ITS-G5, DSRC, comparison, aperiodic, variable size, CAM.

I. INTRODUCTION

V2X (Vehicle to Everything) communications are fundamental for next generation active traffic safety and management applications. V2X communications will extend the awareness range of connected and automated vehicles with information received from neighboring vehicles, the infrastructure or vulnerable road users. Most V2X applications currently rely on broadcasting basic awareness messages (sometimes referred to as beacons). These messages include CAMs (Cooperative Awareness Messages) specified by ETSI or BSMs (Basic Safety Messages) specified by SAE. These messages include basic information such as the position, speed or direction of the transmitting vehicle.

The associate editor coordinating the review of this manuscript and approving it for publication was Yanjiao Chen.

There are currently two main technologies to support first generation V2X communications. IEEE 802.11p was the first V2X technology and is the basis of the DSRC (Dedicated Short Range Communications) and ITS-G5 (specified in Europe by ETSI) standards. There has been extensive testing and trialing worldwide of IEEE 802.11p-based V2X communications and applications. The Third Generation Partnership Project (3GPP) standardized a competing standard under Release 14 and Release 15 based on an adaptation of LTE (Long Term Evolution) for vehicular scenarios. The technology is known as LTE-V2X or Cellular V2X (C-V2X) and is based on the PC5 or sidelink LTE radio interface. This interface allows direct V2V (Vehicle to Vehicle) or V2I (Vehicle to Infrastructure) communications without transferring the data over the cellular network. IEEE 802.11p and LTE-V2X are not interoperable so vehicles will not be able to communicate

with each other if they implement different technologies. This has raised an intense debate on the technology that should be deployed. The debate is not exclusively based on technical aspects but also on regulatory and business ones [1], [2]. This includes for example the allocation of the spectrum (mainly on the ITS 5.9 GHz band) and the capacity to evolve and maintain backwards compatibility with deployed first generation V2X equipment. The social and economic relevance of V2X and the challenges faced if deploying non-interoperable V2X technologies requires a careful evaluation of both technologies under realistic conditions. These evaluations are necessary to support regulatory and business decisions for the best public interest.

Several studies have compared IEEE 802.11p and LTE-V2X. For example, the study reported in [3] presents a complete comparison at the link level. The study shows that LTE-V2X can improve the link budget over IEEE 802.11p by around 7 dB and increase the communication range and reliability at the link level. A complete comparison of both technologies requires though an evaluation at the system level. This is particularly relevant in the case of direct V2X communications if vehicles autonomously select their radio resources. In this case, the design of the MAC (Medium Access Control) can significantly impact the final performance, especially as V2X networks scale. It has already been proven that the MAC of both IEEE 802.11p [4] and LTE-V2X [5] are prone to packet collisions when the channel load increases. Several studies ([2], [6]–[10]) have compared the performance and configuration of IEEE 802.11p and LTE-V2X at the system level. However, existing studies generally consider a simplified traffic model for generating messages. This model was proposed in 3GPP for the evaluation of LTE-V2X [11] but does not follow any of the vehicular standards that define how messages should be generated. The model generates messages periodically, and messages have one or two possible sizes. ETSI and SAE define in [12] and [13], respectively, when awareness messages (CAMs and BSMs) should be generated and what should be their content and size. Several OEMs demonstrated experimentally in [14] that CAMs are not generated periodically and their size constantly varies. The time interval between messages and their size can significantly influence the operation and performance of the MAC in distributed environments where vehicles autonomously select their radio resources. In this context, this study advances the state of the art with an in-depth comparison at the system level of IEEE 802.11p and LTE-V2X mode 4 when considering aperiodic messages of variable size that are generated following the ETSI CAM standard. The study focuses on LTE-V2X mode 4 since it does not require cellular infrastructure support and is hence the baseline mode for ubiquitous active traffic safety. The study also analyses how different message patterns (i.e. periodic or aperiodic and of constant or variable size) can affect IEEE 802.11p and LTE-V2X. This includes evaluating different possible configurations of IEEE 802.11p and LTE-V2X under various traffic densities. The study demonstrates that the sensing-based semi-persistent scheduling scheme defined in LTE-V2X faces significant challenges when handling aperiodic messages and messages of variable size. This study demonstrates that these challenges cannot be resolved with different configurations of LTE-V2X, and IEEE 802.11p outperforms LTE-V2X as the network scales. In particular, IEEE 802.11p achieves better performance under medium and high traffic densities, i.e. when the MAC has a higher impact on the final performance than the physical layer. The study demonstrates that IEEE 802.11p can better cope than LTE-V2X with aperiodic messages and messages of variable size.

II. V2X TECHNOLOGIES

A. IEEE 802.11p

IEEE 802.11p is an evolution of IEEE 802.11a for vehicular communications. IEEE 802.11p uses an OFDM (Orthogonal Frequency Division Multiplexing)-based physical (PHY) layer with a channel bandwidth of 10 MHz. IEEE 802.11p uses the same modulation and coding schemes as IEEE 802.11a. It supports data rates ranging from 3 to 27 Mbps using coding rates 1/2, 2/3 or 3/4 (convolutional coding) and BPSK (binary phase shift keying), QPSK (quadrature phase shift keying), 16-QAM (16-quadrature amplitude modulation) or 64-QAM modulations.

The IEEE 802.11p basic access method is the Distributed Coordination Function (DCF) of IEEE 802.11 that is known as Carrier Sense Multiple Access with Collision Avoidance (CSMA/CA). In CSMA/CA, a node has to sense the radio channel before transmitting a packet. The node will not transmit if another node is using the channel. If the channel is sensed as idle, the node can start its transmission. If the channel is sensed as busy, the node defers its transmission until the end of the current transmission. The radio channel is sensed as busy when the vehicle detects a signal with a received power strength higher than the Clear Channel Assessment (CCA) threshold. The CCA threshold must be higher than the receiver's sensitivity level (or sensing power threshold). At the end of the channel busy period, the node waits for a backoff time to minimize collisions during contention between multiple nodes that also deferred their transmission. This time is calculated for each packet by multiplying the parameter aSlotTime and an integer number that is randomly selected in the interval [0,CW]; CW is referred to as the *Contention Window*. The standard sets CW = aCWmin = 15 and aSlotTime = 13μs for transmitting broadcast packets in 10 MHz channels. The node decreases the backoff time when it senses idle the channel. The node can start its transmission when its backoff time reaches zero.

The capture effect can improve the performance of IEEE 802.11 technologies [15] and it is implemented in many chips. It allows a node to stop receiving a packet if it detects a new packet with significantly higher signal strength. To this aim, the node continuously monitors the received signal strength while in reception mode. If there is suddenly

a sharp increase (e.g. by 10 dB), the receiver stops decoding the packet it was receiving and starts decoding the new packet that is received with higher signal strength. If the capture effect is not implemented, the node will not be able to receive and decode the new packet with higher signal strength and this packet would generate interference. The capture effect can have a strong impact on vehicular networks due to the hidden terminal problem. It is also particularly useful to improve the packet reception probability at short distances.

B. LTE-V2X

LTE-V2X can operate with 10 MHz or 20 MHz channels. LTE-V2X utilizes a time-frequency resource structure (Fig. 1) similar to that of LTE. The time is structured into 1 ms sub-frames that contain 14 OFDM symbols. The channel bandwidth is divided in Resource Blocks (RBs) of 180 kHz each. Each RB is made of 12 OFDM sub-carriers separated by 15 kHz each. RBs within the same sub-frame are organized into sub-channels. LTE-V2X defines different Modulation and Coding Scheme (MCS) using turbo coding and QPSK or 16-QAM. In LTE-V2X, the data and control information are encapsulated in Transport Blocks (TBs) and Sidelink Control Information (SCI), respectively. TBs are transmitted over Physical Sidelink Shared Channels (PSSCH) and SCIs over Physical Sidelink Control Channels (PSCCH) [16]. A TB contains a full packet and can occupy one or more sub-channels depending on the MCS and the number of RBs per sub-channel. Each SCI is associated to a TB and occupies 2 RBs. An SCI contains important information to decode a TB, for example, the utilized MCS, the RBs used to transmit the TB or information related to the reserved sub-channels for the following transmission. The SCI must be correctly received to be able to decode its associated TB. A TB and its associated SCI must be transmitted in the same sub-frame as illustrated in Fig. 1.

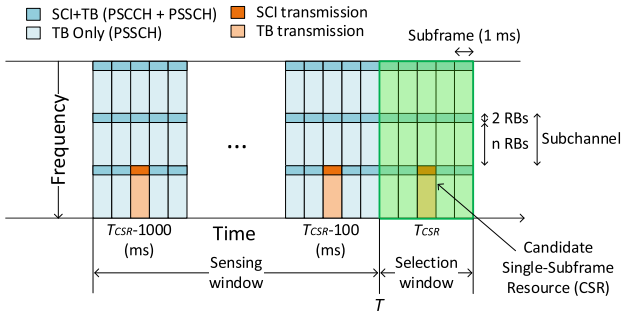

FIGURE 1. LTE-V2X channelization (adapted from [10]).

LTE-V2X can operate under Mode 3 or mode 4. In Mode 3, the cellular base station (or eNB) selects and manages the sub-channels for the direct communication between vehicles. In mode 4, vehicles autonomously select their sub-channels. Vehicles operating under mode 4 need to utilize a common set of parameters so that they can communicate with each other. These parameters include, among others, the number of sub-channels per sub-frame and the number of RBs per sub-channel [17]. These parameters are not fixed by the standard. They can be pre-configured, e.g. using the default values defined by ETSI [18]. Alternatively, they can be configured by the cellular network when vehicles are under cellular coverage.

In LTE-V2X mode 4, vehicles utilize the sensing-based Semi-Persistent Scheduling (SPS) scheme [16], [19] defined in Release 14 to autonomously select their sub-channels. This scheduling scheme is sensing-based and is used by vehicles to identify and select sub-channels that are not occupied by other vehicles. To this aim, the scheduling scheme includes a semi-persistent reservation process that vehicles utilize to notify neighboring vehicles of the selected and reserved sub-channels. In particular, vehicles use the Resource Reservation Interval (RRI) included in the SCI to inform neighboring vehicles when they will utilize the reserved sub-channel(s) for their next transmission. A vehicle that uses a given sub-channel to transmit its current TB (and its associated SCI) at time t will use the RRI to notify nearby vehicles that it plans to use the same sub-channel for its next transmission at t+RRI. The RRI is then used to prevent other vehicles from utilizing the same sub-channel(s). The RRI can be configured equal to 20 ms, 50 ms, 100 ms or any multiple of 100 ms. The 3GPP standard does not fix a value of the RRI and its configuration is up to UE (User Equipment) implementation [19]. The configuration of the RRI has an important impact on the operation of the sensing-based SPS scheme. Its value should be adapted as much as possible to the characteristics of the messages that vehicles must transmit.

Vehicles use the selected sub-channel(s) for a number of consecutive *Reselection Counter* transmissions. *Reselection Counter* is randomly selected between 5 and 15 for RRI = 100 ms (or any multiple of 100 ms). *Reselection Counter* is decremented by one after each transmission, and a new value must be selected every time a vehicle must reserve new sub-channel(s). New sub-channel(s) must be reserved if at least one of the following conditions is satisfied:

- New sub-channel(s) must be reserved with probability $(1 - P)$ if the *Reselection Counter* reaches 0. P can be configured between 0 and 0.8. Increasing P augments the probability to maintain selected sub-channel(s) for longer periods of time. This provides a more stable sensing environment. However, increasing P also augments the probability for persistent packet collisions between two vehicles that select the same sub-channel(s) [20]. If a vehicle does not maintain the current reservation when *Reselection Counter* reaches 0, it notifies other nodes by setting the RRI in the SCI equal to 0.
- New sub-channel(s) must be reserved if the new packet or TB does not fit in the reserved sub-channel(s).
- New sub-channel(s) must be reserved if the current reservation cannot satisfy the latency deadline of a new packet. This happens if the time until the next reserved sub-channel(s) is higher than the latency deadline of the new packet.

The process to select and reserve new sub-channel(s) is referred to as reselections. To select new sub-channel(s) at time T, the ego vehicle executes the following three steps of the sensing-based SPS scheme:

- Step 1. The ego vehicle identifies first the Candidate Single-Subframe Resources (CSRs) within the Selection Window. The Selection Window (Fig. 1) is the time period between T and the latency deadline of the incoming packet (equal or lower than 100 ms [16]). A CSR is a group of adjacent sub-channels within the same sub-frame where the new SCI+TB to be transmitted fits.
- Step 2. The ego vehicle excludes the identified CSRs that it estimates will be used by other vehicles. To this aim, the ego vehicle senses the transmissions from other vehicles during the so-called Sensing Window. The Sensing Window is the time period that includes the last 1000 sub-frames before T (Fig. 1). A CSR is excluded if the two following conditions are met: 1) the ego vehicle has received an SCI from another vehicle indicating that it will utilize this CSR in the current Selection Window or at the same time as the ego vehicle will need it to transmit any of its following *Reselection Counter* transmissions; 2) the ego vehicle excludes a CSR if its average Reference Signal Received Power (RSRP) measured over the TB associated to the corresponding SCI is higher than a given threshold. The RSRP threshold is a configurable parameter. The ego vehicle builds a list L_1 with all the CSRs that have not been excluded. L_1 must include at least 20% of all CSRs in the Selection Window. Otherwise, Step 2 is iteratively executed increasing the RSRP threshold by 3 dB at each iteration until the 20% target is met.
- Step 3. The ego vehicle builds a list L_2 with the CSRs included in L_1 that have the lowest average RSSI (Received Signal Strength Indicator) over all its RBs. This RSSI value is averaged over all the previous T_{CSR}-$T_{IPI}\cdot j$ sub-frames where $T_{IPI} = 100$ ms. The total number of CSRs in L_2 must be equal to 20% of all CSRs in the Selection Window. The ego vehicle randomly selects a CSR from L_2 to transmit its new packet, and it maintains the selection for its next *Reselection Counter* transmissions. We refer to the selected CSR as selected sub-channel(s) in the rest of the paper.

III. IMPACT OF MESSAGE VARIABILITY ON THE OPERATION OF THE LTE-V2X MODE 4 MAC

This study investigates the impact of different message traffic patterns on the operation and performance of IEEE 802.11p and LTE-V2X mode 4. In particular, the study analyses the impact of variable time intervals between messages and message sizes. Section IV presents the message generation models that are utilized for the numerical evaluation of this impact. This section discusses qualitatively the impact that messages of variable size and time intervals can have on the LTE-V2X mode 4 MAC. The section focuses the discussion on LTE-V2X mode 4 because IEEE 802.11p has a simpler but more flexible MAC. IEEE 802.11p does not have a time-frequency structure like LTE-V2X. It also does not utilize a semi-persistent reservation of resources. In IEEE 802.11p, nodes can access the channel at any time if they sense that the channel is free. A node senses the channel prior to transmission for every packet (i.e. there is no reservation). This process is independent of the message size. As a result, the IEEE 802.11p MAC is not really affected by the size of the messages and whether messages are periodic or aperiodic. This is not the case of LTE-V2X since it uses a pre-defined time-frequency structure that conditions the access to the channel as well as the size of packets that can fit in a configured sub-channel. In addition, LTE-V2X semi-persistently reserves the selected sub-channels. This reservation might not be utilized if messages are generated aperiodically. All these aspects are discussed in detail in this section and are numerically quantified in Section VI.

A. RESELECTIONS IN SENSING-BASED SPS

In LTE-V2X mode 4, a vehicle might reselect its sub-channel(s) when *Reselection Counter* is equal to 0 (it depends on P). Reselections can generate packet collisions since neighboring vehicles will not be aware of the new selected sub-channel(s) until the next TB is transmitted. The number of reselections increases with the traffic density, and the probability of packet collisions increases with the number of reselections. This is illustrated in Fig. 2 that represents the time-frequency structure in LTE-V2X. Fig. 2.a depicts a scenario where two vehicles reselect sub-channels at two different time instants T_{resel1} and T_{resel2}. Their transmissions can collide if their Selection Windows overlap and they select the same sub-channel(s) in the time window where the two Selection Windows overlap. If this happens, the collisions will persist until at least one of the two vehicles reselects new sub-channels. The probability of packet collision increases when the number of vehicles reselecting sub-channels increases since there is a higher probability that Selection Windows overlap. This is visible in Fig. 2.b where a third vehicle (V_3)

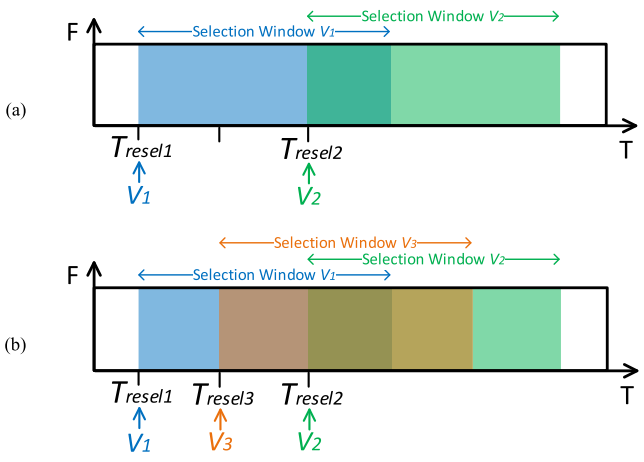

FIGURE 2. Reselections in LTE-V2X and probability of packet collisions.

reselects its sub-channels at T_{resel3} and its Selection Window overlaps with that of V_1 and V_2. This can generate additional packet collisions between V_3 and V_1 and between V_3 and V_2.

B. ADDITIONAL RESELECTIONS

Reselections originated by the depletion of *Reselection Counter* are part of the sensing-based SPS scheme and are hence independent of the message traffic patterns. However, variations in the size of messages (and the corresponding TBs) or the time between messages can generate additional reselections before *Reselection Counter* is depleted. For example, a reselection will occur when a new message has a bigger size than the previous message and it does not fit in the previously reserved sub-channel(s).[1] We refer to this as a size reselection. Size reselections are illustrated in Fig. 3 that represents a scenario where a vehicle generates a first message (or TB) at T_{G1} and reserves two sub-channels for its transmission at T_{R1}. The next message generated at T_{G2} is bigger and does not fit in the two reserved sub-channels at T_{R2}. The vehicle must then reselect new sub-channels to transmit the new message.

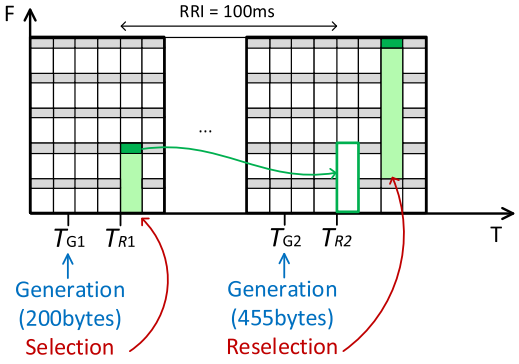

FIGURE 3. Reselection of sub-channel(s) due to variations in the size of messages.

Variations in the time between messages can also force additional reselections that we refer to as latency reselections. This depends on the strategy to select the RRI and on the time interval between messages. In particular, additional reselections can occur when sub-channel(s) are reserved with an RRI larger than the minimum time interval between messages or TBs. This scenario is illustrated in Fig. 4 where a vehicle generates a first TB at T_{G1} and reserves two sub-channels for its transmission at T_{R1}. The selected sub-channels are reserved at $T_{R2} = T_{R1}$+RRI (RRI = 200 ms in Fig. 4) for transmitting the next TB. Let's suppose that the next TB is generated at T_{G2} and has a latency deadline of 100 ms. The vehicle must then transmit the TB before T_{G2}+100 ms. If (T_{G2}+100 ms) < T_{R2}, the vehicle is forced to reselect new sub-channels to transmit the TB before the latency deadline even if *Reselection Counter* is not depleted.

[1]A reselection does not occur if the new message is smaller than the previous message. In this case, some RBs of the selected and reserved sub-channel(s) will be left unused when transmitting the smaller message.

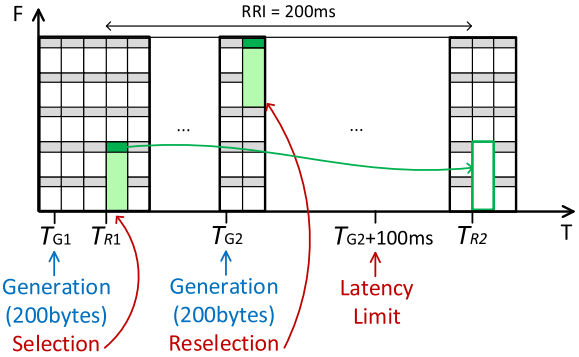

FIGURE 4. Reselection of sub-channel(s) due to variations in the time-interval between messages.

C. UNUTILIZED RESERVATIONS

Reselections due to variations in the size of messages and the time interval between messages can leave previously reserved sub-channel(s) unutilized. However, other vehicles will still think that these sub-channel(s) are reserved and will not consider them as candidate sub-channels. This is visible in Fig. 3 and Fig. 4. In these figures, the reservation of sub-channels at T_{R2} is unutilized because other vehicles believe these sub-channels are still reserved by the transmitting vehicle even though this vehicle had to select new sub-channel(s) at T_{G2}. We refer to this problem as unutilized reservations. Unutilized reservations negatively impact the performance since they effectively reduce the capacity as the number of available sub-channels for other vehicles to select is reduced. This increases the risk of packet collisions when the network load augments.

It should be noted that reselections resulting from depleting the *Reselection Counter* do not generate unutilized reservations. Vehicles transmit their RRI in the SCI associated to a TB. The vehicles that receive the SCI know which sub-channels the transmitting vehicle will utilize to transmit its next TB thanks to the RRI. Before transmitting the last TB that depletes the *Reselection Counter*, the transmitting vehicle evaluates $1 - P$ to decide if it maintains the current reservation or selects new sub-channels. If new sub-channels must be reserved, the RRI is set equal to zero to announce neighboring vehicles that the transmitting vehicle will select new sub-channel(s) for transmitting the following TB. This frees the sub-channel(s) currently utilized by the transmitting vehicle, and these sub-channels can be used by other vehicles thereafter. A vehicle that must reselect its sub-channel(s) before *Reselection Counter* is depleted due to variations in size or time interval of TBs does not set RRI to zero in its last transmission since it cannot anticipate that it would have to reselect new sub-channel(s) for its next TB. As a result, it cannot inform neighboring vehicles that it will not utilize the previously reserved sub-channels.

Reservations can also be left unutilized even if there are no additional reselections. This can occur if the time between messages or TBs is larger than the RRI. This scenario is illustrated in Fig. 5.a where a vehicle V_a generates a first TB

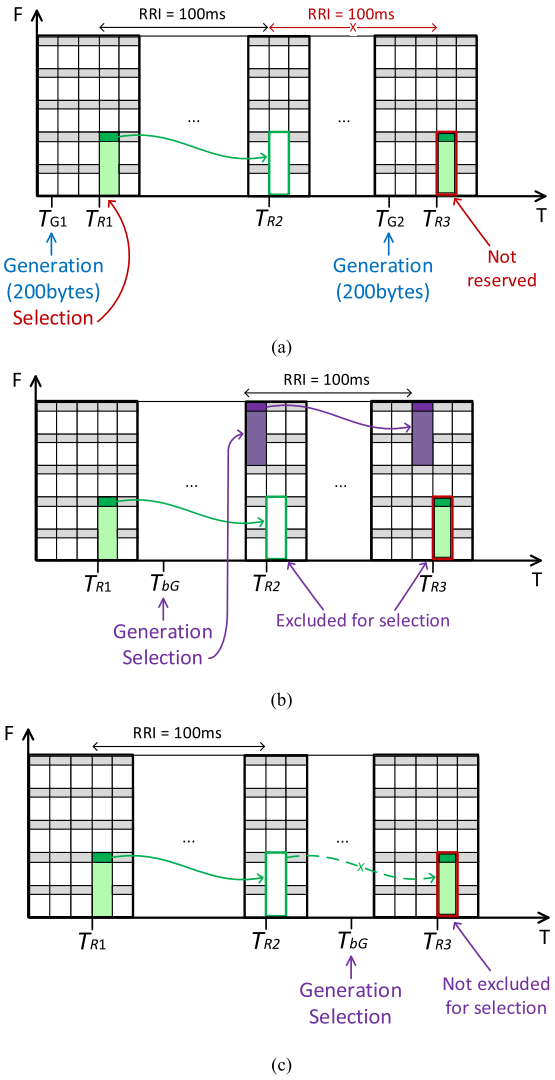

FIGURE 5. Unutilized reservations.

at T_{G1} and reserves two sub-channels for its transmission at T_{R1}. The vehicle reserves the same sub-channels at $T_{R2} = T_{R1}$+RRI. However, the next TB is generated at T_{G2} and $T_{G2} > T_{R2}$. The complete reservation announced for T_{R2} (using the SCI in the first TB) is then left unutilized and all other vehicles cannot use these sub-channels since they are reserved (even if unutilized) by the transmitting vehicle. The vehicle V_a transmits the TB generated at T_{G2} using the same sub-channels at T_{R3} (assuming $T_{G2} + latency\_deadline > T_{R3}$). However, the vehicle has not announced the reservation of the sub-channels at T_{R3} since it did not transmit a SCI (with the corresponding RRI) at T_{R2}. Other vehicles believe then that the sub-channels at T_{R3} are free. Transmitting the second TB at T_{R3} can generate packet collisions with other vehicles that are reselecting sub-channels and may select the sub-channels used by V_a at T_{R3}. This depends on when these other vehicles generate their TB and select new sub-channels. If they do so before T_{R2} (Fig. 5.b), they will exclude as candidate sub-channels the empty reservation from V_a at T_{R2} since they believe that these sub-channels are going to be used by V_a. This is illustrated in Fig. 5.b where a second vehicle V_b generates a first TB at T_{bG}. The vehicle launches then the process to select sub-channels before T_{R2} and excludes the sub-channels reserved by V_a at T_{R2} from its list of candidate sub-channels. V_b will then select different sub-channels than V_a for its first TB and will reserve them for the next TB. There is then no risk of collision between V_a and V_b. The risk of collision exists if V_b generates its TB at $T_{bG} > T_{R2}$ (Fig. 5.c). In this case, V_b believes that V_a will not use the sub-channels at T_{R3} since V_a did not transmit an SCI (and TB) at T_{R2} indicating the reservation using the RRI. Consequently, V_b considers that the sub-channels used by V_a at T_{R3} are available, and a collision would exist if after applying the sensing-SPS scheme V_b selects for its transmissions any of the sub-channels used by V_a at T_{R3}.

D. UNUSED SUB-CHANNEL(S)

Variations in the size of TBs can also result in unused sub-channels even if this variation does not generate an additional reselection. This can occur if the new TB is smaller than the reserved sub-channels. In this case, there will be no additional reselection but some of the reserved sub-channels will be left unused and other vehicles cannot utilize them since they are reserved. This reduces again the number of available sub-channels and increases the risk of packet collisions with the network load. This scenario is illustrated in Fig. 6 where a vehicle generates a first TB at T_{G1} and reserves four sub-channels for its transmission at T_{R1}. The next TB is generated at T_{G2} and only needs two of the four sub-channels. The other two sub-channels are still reserved but left unused by the transmitting vehicle. Other vehicles cannot utilize them since they are reserved by the transmitting vehicle.

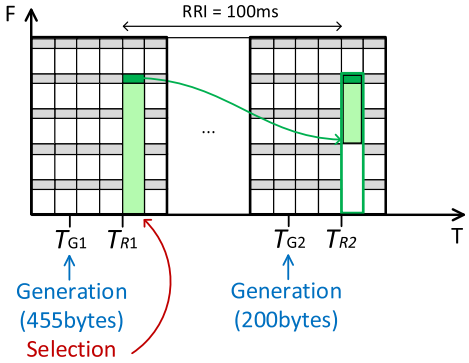

FIGURE 6. Unused sub-channels due to variations in the size of TBs.

IV. MESSAGE GENERATION MODELS

The previous section has shown that the LTE-V2X mode 4 MAC can experience certain challenges when handling aperiodic messages and messages of variable size. It is then important to analyze how different message traffic patterns affect the operation and performance of LTE-V2X and IEEE 802.11p. This section presents the message generation models that have been implemented to conduct this study.

The study focuses on basic awareness messages that are constantly broadcasted by vehicles and support a wide range of V2X applications. These messages include basic information about the transmitting vehicle such as its position or speed. We consider different types of models to generate awareness messages. This goes from simple models that generate messages periodically and of constant size to models that generate messages following the ETSI CAM standard. Different models are considered to analyze the performance under periodic and constant size messages and also under aperiodic messages of variable size. This is done so that our study is not constrained to a specific standard (in particular, the ETSI CAM standard) and our conclusions provide indications for different message types. The implemented models are described in the following sub-sections and their characteristics are summarized in Table 1.

TABLE 1. Message generation models.

MODEL NAME	CAM size	Time-intervals between CAMs
Simplified	Fixed size (200 bytes)	Fixed (200 ms)
3GPP	Four consecutive messages of 190 bytes each followed by one message of 300 bytes	Fixed (200 ms)
Empirical CAM	Following complete empirical CAM model in [26]	Following complete empirical CAM model in [26]
Empirical-size	Following empirical separate size model in [26]	Fixed (200 ms)
Empirical-time	Fixed size (200 bytes)	Following empirical separate time-interval model in [26]

A. SIMPLIFIED MODEL

Many of the studies reported to date consider simple message generation models that do not implement specific standards such as CAM or BSM. Many studies consider a constant message size of 200 Bytes and periodic messages. This is for example the case of the IEEE 802.11p studies reported in [4] and [21] as well as the LTE-V2X studies in [22] and [23]. We have implemented this simplified message generation model for comparison. Our implementation considers messages of constant size (200 Bytes) with a fixed time between messages of 100 ms or 200 ms.

B. 3GPP MODEL

We have also implemented the message generation model utilized by the 3GPP during the LTE-V2X standardization process [11]. This model considers periodic messages with a constant time between messages equal to 100 ms. The model considers two message sizes as follows: four out of five consecutive messages have a constant size of 190 Bytes and the fifth message has a size of 300 Bytes. This pattern is repeated periodically. This model is commonly utilized in the literature to evaluate the performance and efficiency of LTE-V2X (e.g. [24], [25]).

C. EMPIRICAL CAM MODEL

The two previous models are simple but do not generate messages following any specific vehicular message standard such as CAM or BSM. To adequately evaluate the operation and performance of IEEE 802.11p and LTE-V2X, it is necessary to consider models that generate messages following vehicular standards. To this aim, this study focuses on CAMs that have been specified by ETSI in [12]. CAM messages (or CAMs) are generated at the Facilities layer of the ETSI ITS Communications Architecture. Their format and generation rules are defined by ETSI in [12] and are independent of the underlying wireless technology (IEEE 802.11p or LTE-V2X). The generation of CAMs is based on the mobility of the transmitting vehicle. A vehicle checks every $T\_CheckCamGen \leq 100$ ms how much its position, speed and heading has changed since it generated its last CAM. The vehicle generates a new CAM if its position has changed more than 4 m, its speed has changed more than 0.5 m/s or its heading has changed more than 4° [12]; the speed and heading variations are computed as absolute values. A CAM is also generated if the time elapsed since the last generated CAM is equal to or higher than 1 s. It should be noted that the time between CAMs is variable and a multiple of *T_CheckCamGen*. In particular, the time between CAMs depends on the mobility of vehicles, and vehicles will generate more CAMs per second when their speed or acceleration is higher. Current CAM generation rules establish that CAM messages are not necessarily periodic. In fact, the measurements reported in [14] show that it is unlikely that the time between consecutive CAMs is constant for more than 3 CAM messages, except when the vehicle is stopped.

The size of CAM messages is not constant either. A CAM includes one ITS PDU header, one basic container and one high frequency container [12]. The basic container includes information about the transmitting vehicle such as its position. The high frequency container contains dynamic information such as the acceleration, heading or speed of the transmitting vehicle. Optionally, a CAM can also include one low frequency container and one special vehicle container. The size of each CAM depends on the optional containers and the optional data elements included in each container. For example, the high frequency container is mandatory but its size is variable because 7 of its 16 data elements are optional. Security certificates also have an impact on the amount of data that is finally transmitted and they are not included in all CAMs [14]. The size of CAMs is therefore variable and depends on the vehicular context and the implementation (e.g. how the vehicle's path history is coded in the optional low frequency container) [14].

An accurate evaluation of IEEE 802.11p and LTE-V2X requires the use of a CAM generation model that accurately represents the variation in size and time between messages included in the CAM format and generation rules specified by ETSI. To this aim, this study utilizes a realistic CAM generation model presented in [26]. This model was derived from a set of empirical measurements collected by two OEMs

that implemented the ETSI CAM standard in their on-board units. The traces were captured in real driving conditions in a highway scenario close to Gifhorn (Germany). The model produces CAM messages with variable size and time between messages following the mobility-based rules specified in ETSI. In particular, we utilize the Volkswagen-Highway empirical model reported in [26] and provided open-source by the authors. We refer to this model as the *Empirical CAM model*. This model was created by the authors from the analysis of real traces presented in [14] and collected by Volkswagen in highway scenarios. The traces were collected with equipment implementing the CAM standard, in particular the CAM Facilities layer *C2C-CC profile 1.3* [14]. The model is based on *m*th order Markov sources and models the size of CAMs and the time interval between CAMs. The model is able to capture the cross-correlation present between the size of each CAM and the time interval to the next CAM as demonstrated in [26]. The model also models the correlation existing between the current CAM and the previous five CAMs [26]. The model follows the CAM standard and therefore checks every *T_CheckCamGen* whether a CAM message should be generated. *T_CheckCamGen* was set equal to 100 ms during the trials where the traces were collected. CAMs were then generated at multiples of 100 ms at the Facilities layer. However, a random jitter was observed (with zero mean and standard deviation of 3.235 ms) due to several factors including the time needed to process and encode the CAMs, and the time spent in executing other tasks on the hardware. Consequently, CAMs were not sent down to the lower layers at multiples of 100 ms. This jitter is also included in the model. The study in [26] demonstrates that the *Empirical CAM model* is able to generate CAM messages with sizes and time intervals between CAMs that accurately mimic the empirical traces described in [14]. The traces were collected under realistic highway traffic conditions where vehicles accelerate, decelerate, change lanes, enter/leave the highway, etc. The *Empirical CAM model* allows us generating CAMs with the variability resulting from the application of ETSI standards in real driving conditions such as those in [14]. It is important to emphasize the high variability of the size of CAMs and the time between CAMs present in the traces and modeled in the implemented *Empirical CAM model*. This variability is illustrated in Fig. 7 and Fig. 8. Fig. 7 plots a sample of the traces collected by Volkswagen in a highway and presented in [14]. The sample shows the variability of the size of CAMs and the time between CAMs. Fig. 8 plots the PDF (Probability Density Function) of the CAM sizes and time intervals between CAMs from the traces collected in the trials. The figure clearly shows that CAM messages are not periodic and their size is not constant. The implemented *Empirical CAM model* accurately matches the variability illustrated in Fig. 7 and Fig. 8. Modelling this variability is critical to accurately evaluate the performance of IEEE 802.11p and LTE-V2X in realistic conditions when implementing ETSI standards. The variability present in the generation of CAMs can impact differently IEEE 802.11p

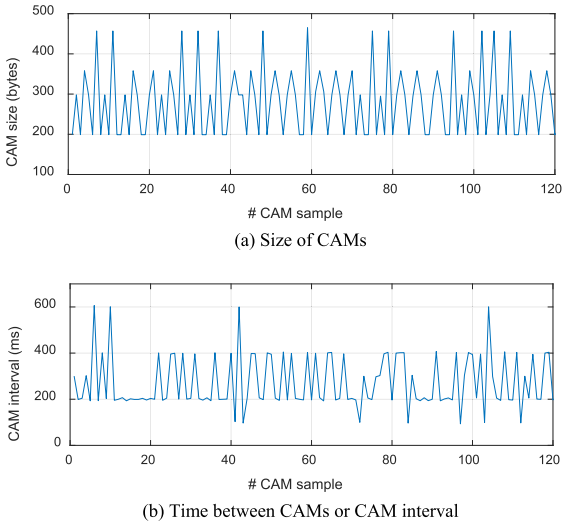

(a) Size of CAMs

(b) Time between CAMs or CAM interval

FIGURE 7. Sample of the empirical traces presented in [14] and collected by Volkswagen in a highway.

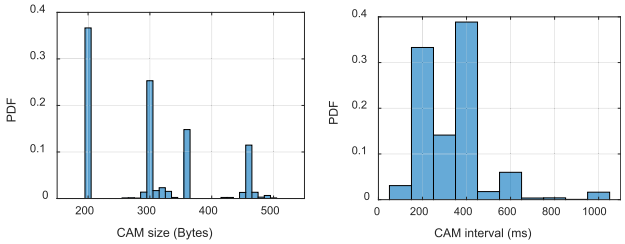

FIGURE 8. PDF of the size of CAMs and the time intervals between CAMs obtained from the traces collected and presented in [14].

and LTE-V2X since they implement different MAC protocols. Reference [14] also presents traces collected by Volkswagen in urban scenarios. These traces show that CAM messages exhibit variability in size and time interval as observed in highway scenarios. This variability is at the origin of the results and trends presented in this paper. The conclusions derived for highway scenarios could hence also be extended to urban scenarios.

D. EMPIRICAL SEPARATE MODELS

The *Empirical CAM model* allows analyzing how IEEE 802.11p and LTE-V2X handle the transmission of aperiodic messages of variable size generated following the ETSI CAM standard. It is also interesting to understand which effect (variable size or time between messages) has a higher impact on the operation and performance of both V2X technologies. To this aim, we utilize variations of the *Empirical CAM model* (see Table 1) where we fix one of the parameters (size or time between messages) and the other parameter is modelled following the principles of the *Empirical CAM model*. These separate models are also presented in [26]. We refer to as *Empirical-size* the model that fixes the time interval between CAMs and models the variability of the size of CAMs. Similarly, we refer to as *Empirical-time* the model that fixes the size of CAMs and models the variability present in the time between CAMs.

V. SIMULATION ENVIRONMENT

We use simulations to compare IEEE 802.11p and LTE-V2X mode 4. In particular, we use the Veins simulation framework that integrates the network simulator OMNET++ and the road traffic simulator SUMO. We have implemented the LTE-V2X mode 4 radio interface following the 3GPP standards [27]. The implementation was validated in [28]. We have also evolved the IEEE 802.11p radio interface available in OMNET++ to include the capture effect. In addition, we have implemented over OMNET++ all the CAM generation models previously described.

A. SIMULATION SCENARIO

This study considers a 5km highway scenario. Statistics are only collected from vehicles located in the center 2km to avoid border effects. We model four different traffic densities:

- *60 veh/km*. In this case, the scenario has 3 lanes in each driving direction and the vehicles' speed is 140 km/h. This scenario corresponds to the *Highway Fast* scenario defined by the 3GPP in [11].
- *120 veh/km*. This scenario has 3 lanes per driving direction but the vehicles' speed is 70 km/h due to the higher traffic density. This scenario corresponds to the *Highway Slow* scenario defined by the 3GPP in [11].
- *200 veh/km*. This scenario has 3 lanes per driving direction and the vehicles' speed is 70 km/h.
- *400 veh/km*. This scenario considers 5 lanes per driving direction and the vehicles' speed is 70 km/h.

All four scenarios correspond to a service level C according to the Highway Capacity Manual [29], i.e. vehicles can drive with speeds close to the free flow speed but freedom to maneuver within the traffic stream is restricted.

B. CONFIGURATION OF IEEE 802.11p AND LTE-V2X

IEEE 802.11p and LTE-V2X are configured to operate over a 10 MHz channel in the 5.9 GHz frequency band. Following the 3GPP simulation guidelines in [11], we model the pathloss using the WINNER+ B1 model with an antenna height of 1.5 m for transmitter and receiver. The shadowing effects are modeled using a log-normal distribution with zero mean and a standard deviation of 3 dB. Spatial shadowing correlation is modeled following the 3GPP guidelines in [11], with a decorrelation distance of 25 m. The PHY layer performance of IEEE 802.11p and LTE-V2X is modeled using BLER (Block Error Rate)-SINR (Signal to Interference plus Noise Ratio) curves from [3] where both technologies are evaluated under the same conditions (including the fast fading model specified in [30]). The curves in [3] report a better PHY layer performance of LTE-V2X compared to IEEE 802.11p; LTE-V2X requires around 3 dB less SINR to achieve the same BLER performance than IEEE 802.11p. Simulations are also conducted using the same PHY layer performance (in particular, the one for LTE-V2X) for both technologies. The objective is to analyze how the two technologies compare if the IEEE 802.11p PHY layer performance is significantly improved as claimed in [31].

IEEE 802.11p and LTE-V2X are configured to transmit at 23 dBm and use the same Modulation and Coding Scheme (QPSK with coding rate of 0.5, i.e. MCS 6 in the case of LTE-V2X). However, different sensitivity levels are considered for each technology. Simulations have been conducted using the minimum sensitivity levels defined in the corresponding standards: −90.4 dBm for LTE-V2X [32] and −85 dBm for IEEE 802.11p [33]. Simulations have also been conducted with better sensitivity levels corresponding to those achieved by commercial devices or prototypes; these values are used as baseline in this study. In particular, we utilize for LTE-V2X the sensitivity level of the prototype in [34]: −103.5 dBm. For IEEE 802.11p, we consider a sensitivity level of −92 dBm that can be easily reached by commercial devices [35].

Two important parameters to be configured in IEEE 802.11p are the *Capture Effect* and *Clear Channel Assessment* (CCA) thresholds. The capture effect is generally implemented in IEEE 802.11 chipsets [15]. The minimum increase in received signal strength to abandon the current frame and start receiving a new frame (capture effect threshold) is normally set to 10 dB [15]. Fig. 9 shows the impact of the capture effect on the PDR (Packet Delivery Ratio) of IEEE 802.11p. The figure has been obtained considering the *Empirical CAM model* and two traffic densities. The figure clearly shows that the capture effect significantly improves the reliability of IEEE 802.11p, especially at short distances. The capture effect is then modeled in this study given its widespread implementation and the positive effect on the performance of IEEE 802.11p. The impact of the CCA on the PDR of IEEE 802.11p is shown in Fig. 10. The figure shows that the lower the CCA threshold, the higher the PDR. We then configure in our study the CCA threshold 0.5 dB higher than the sensitivity level (minimum standard value or commercial reference) used in IEEE 802.11p.

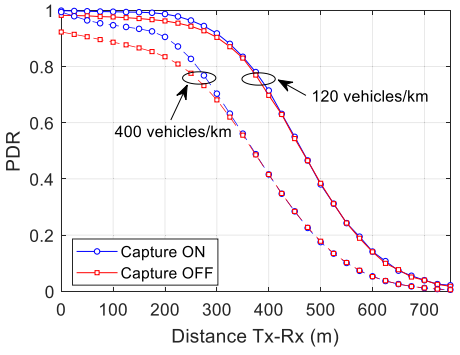

FIGURE 9. PDR of IEEE 802.11p with and without capture effect.

We configure LTE-V2X with 5 sub-channels per subframe following the ETSI recommendations in [18]. Each sub-channel has 10 RBs and we consider the adjacent PSCCH-PSSCH configuration (i.e. a TB and its associated SCI are transmitted in adjacent RBs). Table 2 shows the number of sub-channels needed to transmit CAMs of different

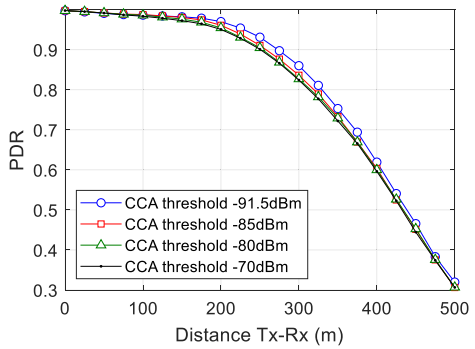

FIGURE 10. PDR of IEEE 802.11p with different CCA threshold values.

TABLE 2. Sub-channels per packet size in LTE-V2X.

Packet size (bytes)	CAM model	Number of sub-channels
190	3GPP	2
200	Simplified, Empirical CAM, Empirical-time	2
300	3GPP, Empirical CAM, Empirical-size	3
360	Empirical CAM, Empirical-size	3
455	Empirical CAM, Empirical-size	4

sizes considering the configured sub-channelization and the use of MCS 6 (i.e. QPSK with coding rate of 0.5). The reported CAM sizes correspond to those used in the different CAM message generation models.

The RSRP threshold has been configured with a low value (−140 dBm) so that the sensing-based SPS scheme excludes all sub-channels for which an SCI from another vehicle is correctly received. Reference [20] showed that this is the best configuration of the RSRP threshold since Step 2 of the sensing-based SPS scheme is more effective than Step 3 in excluding the sub-channels that are more likely to experience high interference levels. The conclusions in [20] were achieved with the *Simplified model* and the *3GPP model*. We have replicated the analysis presented in [20] with the simulation conditions of this study and with all different message generation models. The same conclusions as in [20] have been obtained with the *Simplified model* and the *3GPP model*: the best performance is achieved with a low value (−140 dBm) of the RSRP threshold. This is visible in Fig. 11 that shows the PDR achieved with different values of the RSRP threshold, two traffic densities and the *Simplified model*. The analysis conducted with the *Empirical CAM model* has shown that in this case the lowest value of the RSRP threshold (−140 dBm) does not always achieve the best performance. This is due to the challenges experienced by LTE-V2X under the presence of aperiodic messages of variable size. These challenges affect the efficiency of Step 2 of the Sensing-Based SPS to adequately exclude the sub-channels that are more likely to experience high interference levels. Our analysis has shown that the optimum value of the RSRP threshold depends on the traffic density. However, the differences observed between the different values of the

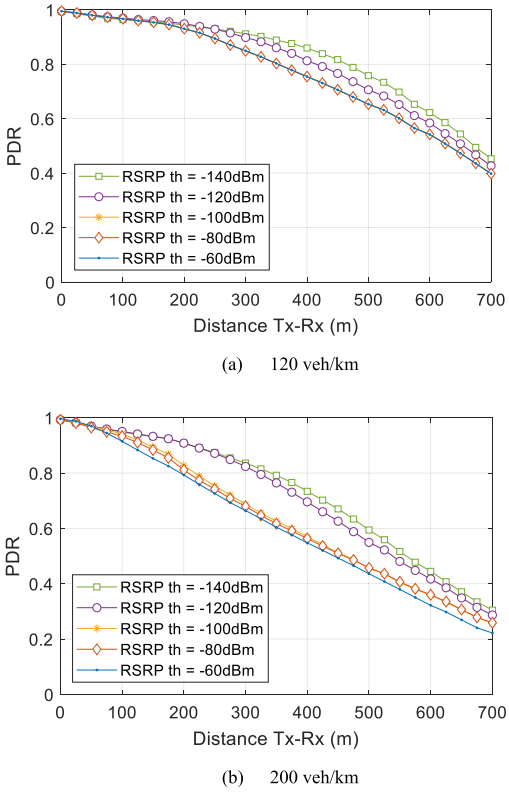

FIGURE 11. Impact of the RSRP threshold with the *simplified model.*

RSRP threshold are small and not significant. This is visible in Fig. 12 that plots the PDR achieved with different values of the RSRP threshold, two traffic densities and the *Empirical CAM model*. The figure also shows that the differences observed are so small that the selection of the RSRP threshold does not affect the comparison between LTE-V2X and IEEE 802.11p. We have set the RSRP threshold to −140 dBm considering the trends observed for the different models and densities.

The probability P to maintain the same sub-channel(s) when the *Reselection Counter* is depleted is set equal to 0 following [20]. Increasing P does not significantly improve the performance but can produce packet collisions that persist over longer periods of time. However, we also analyze in this study $P = 0.8$ to verify that the trends are confirmed for different values of P. LTE-V2X is configured without packet retransmissions since they tend to overload the channel and reduce performance. Nevertheless, we also analyze the impact of packet retransmissions for low traffic densities where the risk to overload the channel is smaller.

A key parameter in the configuration of LTE-V2X is the selection of the RRI. In this study, we set the RRI equal to the time interval between messages when this interval is constant (e.g. in the *Simplified model* and the *3GPP model*). However, to the authors' knowledge, there is no study that has identified the optimum value of the RRI, or the optimum method to configure the RRI, when the time between messages is not constant. In this case, we propose and evaluate the

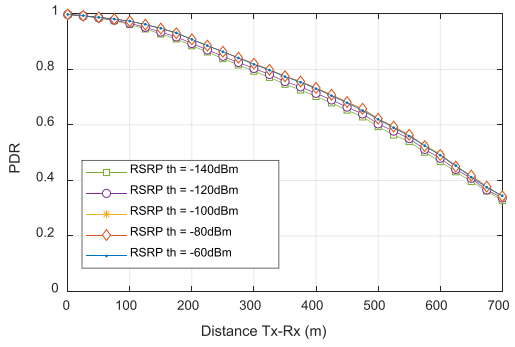

(a) 120 veh/km

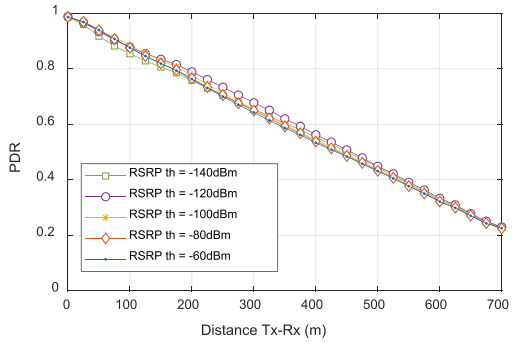

(b) 200 veh/km

FIGURE 12. Impact of the RSRP threshold with the *empirical CAM model.*

performance of LTE-V2X considering three different strategies to configure the RRI:

- Strategy 1: RRI is fixed and equal to 100 ms since 100 ms is the minimum time interval between CAMs.
- Strategy 2: RRI is fixed and equal to 200 ms since 200 ms and 400 ms are the most frequent time intervals between CAMs in the traces used to create the *Empirical CAM model* (72% of the transmissions used one of these two time intervals).
- Strategy 3: RRI is set equal to the time interval of the last CAM generated. This strategy is chosen since it was observed for 50% of the transmissions recorded in the empirical traces that the following time interval was equal to the previous one.

C. METRICS

The performance and operation of IEEE 802.11p and LTE-V2X is compared using several metrics. The performance is mainly estimated by means of the Packet Delivery Ratio (PDR) and the Packet Inter-Reception (PIR). The PDR is the average ratio of packets correctly received to the total number of transmitted packets. It is represented as a function of the distance between the transmitting and receiving vehicles. The PIR is the time between two consecutive packets (transmitted by the same vehicle) that are correctly received. The PIR is used to monitor errors resulting from persistent packet collisions. To this aim, we represent the PIR as a cumulative distribution function (CDF) of all transmissions between vehicles that are at a maximum distance of 100 m. This short distance is chosen to be able to observe errors resulting from persistent packet collisions. Choosing larger distances would also include errors resulting from propagation effects and it will be more challenging to observe the impact of persistent packet collisions.

We also estimate the average ratio of packets lost due to propagation errors and packet collisions.[2] These ratios are also shown as a function of the distance between transmitting and receiving vehicles. The metric *Propagation error* estimates the average ratio of packets lost because they are received with a signal strength below the sensitivity level or because the SNR (Signal to Noise Ratio) is too low to correctly decode the packet. The metric *Collision error* estimates the average ratio of packets lost due to packet collisions. This error occurs when packets collide and a packet cannot be correctly decoded because the SINR is too low due to the interference generated by other vehicles. For IEEE 802.11p, this metric also includes the packets that a receiver discards because it is receiving at the same time another packet and the capture effect threshold is not surpassed.

Another important metric is the *Channel Busy Ratio* (CBR). This metric is used to estimate the channel load. In IEEE 802.11p (Fig. 13.a), it is computed as the ratio of time that the channel is sensed as busy (i.e. the RSSI is higher than the CCA threshold). In LTE-V2X (Fig. 13.b), the CBR is the ratio of sub-channels that experience an RSSI higher than a threshold to the total number of sub-channels in the observation time window. For IEEE 802.11p, the RSSI threshold is set up 0.5 dB higher than the sensitivity level.

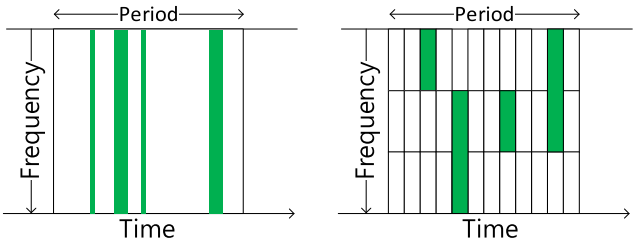

(a) IEEE 802.11p (b) LTE-V2X

FIGURE 13. Estimation of the CBR.

We also compute metrics to quantify the challenges experienced by the LTE-V2X mode 4 sensing-based SPS scheme when transmitting aperiodic messages of variable size. In particular, we compute the following metrics:

- *Counter reselection ratio*. Ratio of messages for which there is a reselection due to the depletion of the *Reselection Counter* to the total number of messages generated.
- *Size reselection ratio*. Ratio of messages that produce a size reselection to the total number of messages generated.

[2]We also estimated the percentage of packet lost due to half duplex errors and the loss of the SCI in LTE-V2X. Few packets were lost due to these types of errors in the conducted simulations, and we omit them in this study.

- *Latency reselection ratio*. Ratio of messages that produce a latency reselection to the total number of messages generated.
- *Total reselection ratio*. Ratio of messages that produce a reselection (counter, size or latency) to the total number of messages generated. It should be noted that this ratio is not equal to the sum of the other three ratios since it is possible that a message generates several types of reselections and this is counted as a single reselection when computing the total reselection ratio.
- *Ratio of unused sub-channels*. Average ratio of unused sub-channels in the reserved sub-channels used to transmit a message or TB.
- *Ratio of unutilized reservations*. Average ratio of reservations that are completely left unutilized (i.e. no sub-channels in the reservation are used) to the total number of reservations. This metric only accounts for unutilized reservations that are not due to an additional reselection since additional reselections are already considered in the size and latency reselection ratios.

VI. COMPARISON OF IEEE 802.11p AND LTE-V2X

A. PERIODIC MESSAGES

The performance of IEEE 802.11p and LTE-V2X is first compared considering periodic messages using the *Simplified model* and the *3GPP model*. Fig. 14 compares the PDR achieved when messages are periodic and of constant size (i.e. *Simplified model* in Section IV.A). Messages are generated every 200 ms so LTE-V2X is configured with the second strategy to select the RRI (i.e. RRI = 200 ms). The results are depicted for four traffic densities and have been obtained considering the baseline parameters specified in Section V.B.

Fig. 14.a shows that under low traffic densities LTE-V2X outperforms IEEE 802.11p. Low traffic densities generate a low channel load (Table 3). When the channel load is low, the MAC has a low impact on the PDR compared to the physical layer. This is actually visible in Fig. 15 that shows the percentage of packets lost due to packet collisions and propagation errors.[3] The figure shows that most packet errors under low traffic densities are due to propagation effects. Under low traffic densities, only a few packets are lost due to packet collisions.

The figure also shows that IEEE 802.11p increases the percentage of packets lost due to propagation errors compared to LTE-V2X since LTE-V2X has a better physical layer in the selected baseline configuration. This explains why LTE-V2X outperforms IEEE 802.11p at medium and large distances. IEEE 802.11p achieves a slightly higher PDR at short distances thanks to the capture effect. LTE-V2X suffers some packet collisions at short distances even if the traffic density is low. These collisions are caused by the reselections that are part of the sensing-based SPS scheme and that can occur

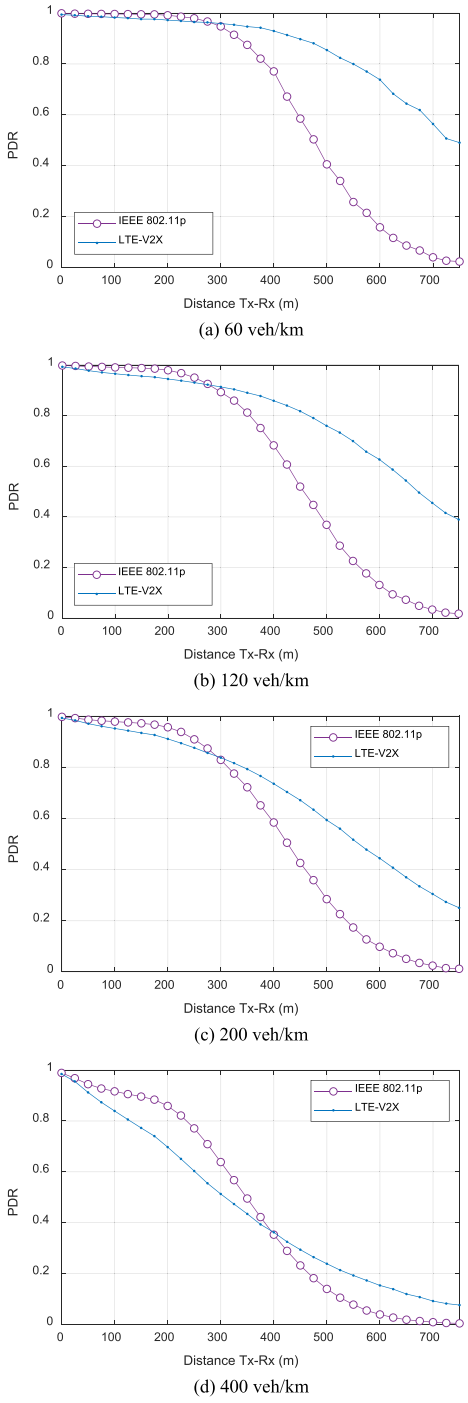

FIGURE 14. PDR experienced with periodic messages (every 200 ms) of constant size (*simplified model*).

when several vehicles select new sub-channels around the same time because their *Reselection Counter* reached zero (Fig. 2). The *counter reselection ratio* is equal to 0.1 in this scenario.[4] This type of collisions is particularly present between vehicles at short distances since these vehicles will

[3] Fig. 15 does not represent the percentage of LTE-V2X packets lost due to half-duplex errors or an incorrect reception of the SCI since they were negligible.

[4] *Reselection Counter* is randomly selected between 5 and 15. The average value is then 10, i.e. a reselection due to the depletion of *Reselection Counter* for 1 out of every 10 packets.

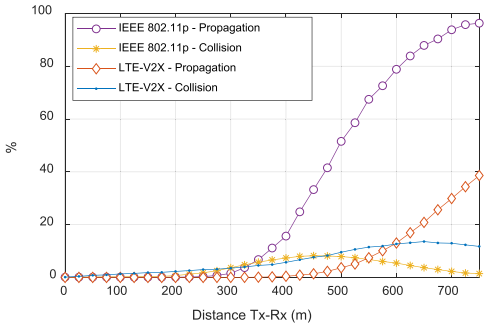

a) 60 veh/km

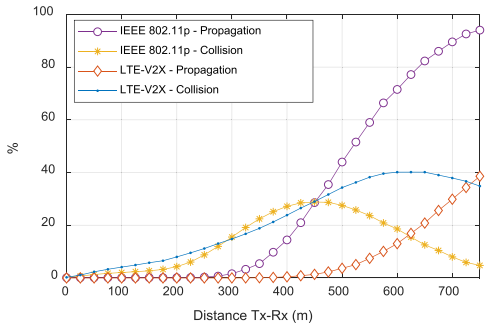

b) 200 veh/km

FIGURE 15. Percentage of packets lost due to propagation and collision errors when messages are periodic and of constant size (*simplified model*).

sense similar RSRP and RSSI levels at all sub-channels when executing the sensing-based SPS scheme. Vehicles at short distances might then select the same sub-channels in their lists L_2 (Section II.B) which increases the risk of packet collisions. This effect is analyzed in detail in [28].

Fig. 14 shows that IEEE 802.11p and LTE-V2X see their PDR degrade when the load increases. The degradation observed for IEEE 802.11p is due to the increase of the CBR (Table 3) that augments packet collisions due to the hidden terminal problem. This is visible in Fig. 15 that shows how the percentage of packets collisions increases with the load for IEEE 802.11p. LTE-V2X is also prone to the hidden terminal effect since SPS is sensing-based. This is reflected in Fig. 15 that also shows how packet collisions increase with the traffic density (and channel load) for LTE-V2X as well. However, the increase is higher for LTE-V2X that sees its performance degrade more strongly under the highest traffic densities (Fig. 14.d). This is the case because packet collisions in LTE-V2X are not only caused by the hidden terminal effect but also by the reselections that are part of the sensing-based scheme. These reselections can occur when *Reselection Counter* is depleted. The risk of packet collisions due to these reselections increases with the traffic density as discussed in Section III.A and illustrated in Fig. 15. This is why packet collisions increase more with the traffic density for LTE-V2X than IEEE 802.11p even for periodic messages of constant size.

Fig. 14 has been obtained considering the *Simplified model* for the generation of messages. This model creates periodic

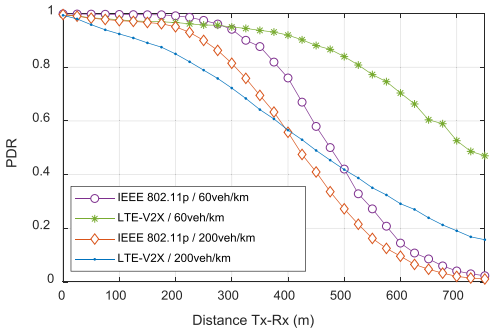

FIGURE 16. PDR experienced with periodic messages of two sizes (*3GPP model*).

messages of constant size. Fig. 16 compares the PDR achieved when considering the *3GPP model* for two traffic densities. This model does not abide to any particular V2X standard (e.g. ETSI or SAE standards) and creates periodic messages of two possible sizes. The time interval between messages has been set constant and equal to 200 ms. LTE-V2X is then configured with the RRI equal to 200 ms. Fig. 14 and Fig. 16 cannot be directly compared because different traffic models result in different average CBR levels even for the same traffic density.[5] However, the same trends are observed for the two figures under low traffic densities, i.e. LTE-V2X outperforms IEEE 802.11p (except for short distances) due to the better physical layer. Fig. 16 shows a higher degradation than Fig. 14 for LTE-V2X compared to IEEE 802.11p under a traffic density of 200 veh/km. In fact, IEEE 802.11p outperforms LTE-V2X except for large distances (again due to higher impact of the physical layer at large distances). The difference is not due to the different CBR levels but mainly to the introduction of two message sizes with the *3GPP model*. As explained in Section III.B, variable message sizes introduce additional reselections. These additional reselections increase the risk of packet collisions in LTE-V2X as the traffic density increases. For the *3GPP model*, the size reselection ratio is equal to 0.062 and the counter reselection ratio is equal to 0.084.[6] The *3GPP model* results in a total reselection ratio of 0.146 compared to 0.1 for the *Simplified model* that only experiences reselections due to the depletion of the *Reselection Counter*. The risk of packet collisions increases with the number of reselections when the traffic density augments. The *3GPP model* also results in an average ratio of unused sub-channels equal to 0.307. Unused sub-channels reduce the efficiency of LTE-V2X when transmitting messages of different sizes that require a different number of sub-channels.

[5]The *3GPP model* results in a CBR equal to 0.13 and 0.131 for LTE-V2X and IEEE 802.11p when the density is 60 veh/km. These values increase to 0.395 and 0.41 respectively. The *3GPP model* results in slightly higher CBR levels than the *Simplified model* due to the introduction of a larger message size.

[6]This value is not equal to 0.1 because if a new sub-channel(s) is selected for a message of small size when *Reselection Counter* is depleted, the selected sub-channel(s) will not be maintained for all following *Reselection Counter* transmissions since a message of bigger size will be generated before the counter is depleted and an additional reselection will be necessary.

B. APERIODIC MESSAGES OF VARIABLE SIZE

Fig. 17 compares the PDR achieved by IEEE 802.11p and LTE-V2X when transmitting aperiodic messages of variable size using the *Empirical CAM model* (Section IV.C). It should be reminded that the *Empirical CAM model* generates CAM messages following the ETSI standard. Fig. 17 has been obtained under the same simulation conditions as Fig. 14.

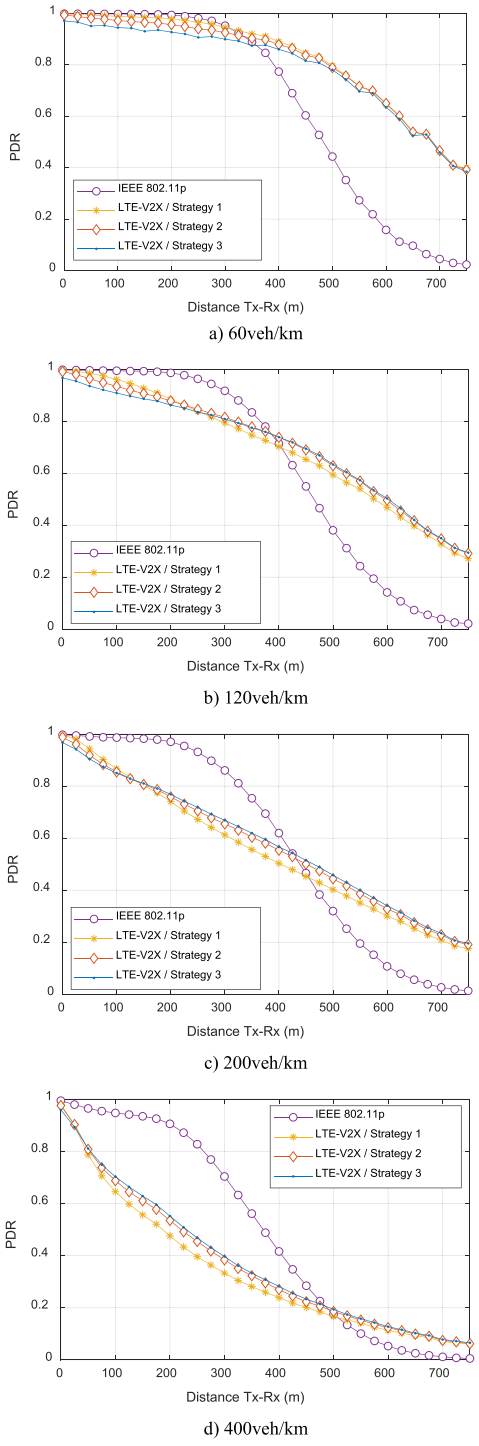

FIGURE 17. PDR experienced with aperiodic messages of variable size (*Empirical CAM model*).

However, Fig. 17 includes the evaluation of the different strategies to select the RRI since messages are aperiodic with the *Empirical CAM model*.

Fig. 17.a and Fig. 14.a show that similar trends are observed with both models under low traffic densities. LTE-V2X outperforms IEEE 802.11p at medium and large distances due to its better physical layer. However, IEEE 802.11p slightly outperforms LTE-V2X at short distances due to the capture effect and the reselections embedded in the design of the LTE-V2X sensing-based scheme that affect vehicles at short distances.

Fig. 17 shows that the PDR also degrades when the load increases. However, the comparison of Fig. 17 and Fig. 14 shows that the degradation is significantly higher for LTE-V2X than IEEE 802.11p when messages are aperiodic and of variable size (*Empirical CAM model*) compared to when messages are periodic (*Simplified model* and *3GPP model*). In fact, Fig. 17 shows that IEEE 802.11p significantly outperforms LTE-V2X when the traffic density (and channel load) increases under the presence of aperiodic messages. The higher degradation with the load observed in Fig. 17 (*Empirical CAM model*) than in Fig. 14 (*Simplified model*) for LTE-V2X compared to IEEE 802.11p is due to the significant impact of aperiodic messages of variable size on the operation and performance of LTE-V2X. This impact is smaller on IEEE 802.11p. IEEE 802.11p is mainly affected by the hidden terminal problem when the load increases independently of whether messages are periodic or aperiodic and whether they are of constant or variable size. On the other hand, LTE-V2X is affected by the hidden terminal problem and the challenges explained in Section III when handling aperiodic messages of variable size. The effect of these challenges is visible when comparing Fig. 18 and Fig. 15. The comparison shows that the difference in terms of percentage of packets lost due to collisions between LTE-V2X and IEEE 802.11p increases more with the load when messages are aperiodic than when they are periodic. Periodic messages only generate reselections due to the depletion of the Reselection Counter. These reselections are also present with aperiodic messages of variable size. However, aperiodic messages of variable size also generate the additional reselections explained in Section III.B. The risk of packet collisions increases for LTE-V2X with the load when the total number of reselections increases. This number is higher with aperiodic messages of variable size than with periodic messages. In addition, variations in the size of messages or the time interval between messages increase the number of unused sub-channels and unutilized reservations. This also increases the risk of packet collisions since it reduces the number of available sub-channels and hence increases the probability that two vehicles will select the same sub-channel(s). All these factors are analyzed in detail in the next sub-section. These factors explain why LTE-V2X experiences more packet collisions than IEEE 802.11p, and why packet collisions increase more in LTE-V2X with aperiodic messages of variable size than with periodic messages. It should be noted that the increase of

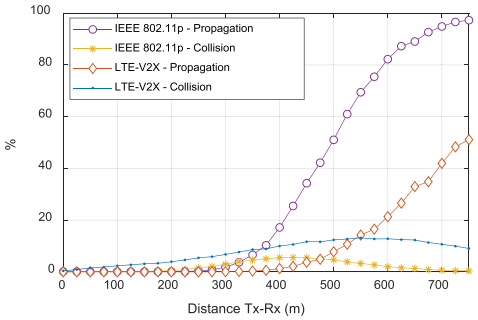

a) 60 veh/km

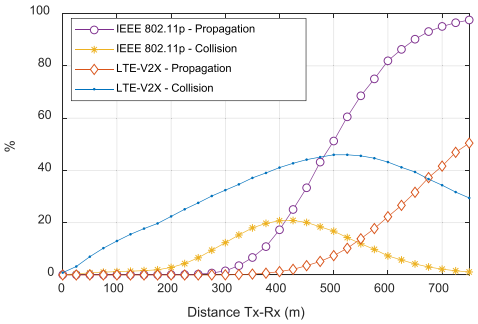

b) 200 veh/km

FIGURE 18. Percentage of packets lost due to propagation and collision errors when messages are aperiodic and of variable size (*empirical CAM model*).

packet collisions in LTE-V2X when messages are aperiodic explains why a lower CBR is measured in LTE-V2X with aperiodic messages than with periodic messages for the same traffic density (Table 3). An increase of packet collisions reduces the CBR since two packets that collide generate half the channel load than they would generate if they do not collide. This also influences the fact that LTE-V2X experiences lower CBR levels than IEEE 802.11p for the same traffic density, in particular when messages are aperiodic (*Empirical CAM model*).

TABLE 3. Channel busy ratio (CBR).

Model	Density (veh/km)	IEEE 802.11p	LTE-V2X
Simplified (200 ms period)	60	0.12	0.119
	120	0.233	0.237
	200	0.376	0.386
	400	0.654	0.638
Empirical CAM	60	0.101	0.095
	120	0.206	0.186
	200	0.334	0.289
	400	0.61	0.485

C. ANALYSIS OF THE OPERATION OF LTE-V2X

This section analyzes the operation of LTE-V2X to better understand the trends discussed in the previous sections and the degradation of LTE-V2X under the presence of aperiodic messages of variable size. This includes an evaluation of the impact on LTE-V2X of the strategies to select the RRI.

TABLE 4. Reselection rates (empirical CAM model).

RRI strategy	Latency reselection	Size reselection	Counter reselection	Total reselection
1	0.001	0.076	0.081	0.155
2	0.169	0.134	0.047	0.313
3	0.234	0.169	0.03	0.387

Table 4 shows the ratio of reselections[7] when transmitting aperiodic messages of variable size (*Empirical CAM model*). Reselections can occur because: 1) *Reselection Counter* reaches zero (counter reselection ratio); 2) a new message does not fit in the reserved resources (size reselection ratio); or 3) new resources must be selected to meet the latency deadline of a new message (latency reselection ratio). If there were no additional reselections (e.g. when considering the *Simplified model*), reselections would only be generated when *Reselection Counter* reaches zero. In this case, the total reselection ratio would be equal to 0.1 since *Reselection Counter* is uniformly distributed between 5 and 15 and there would then be a reselection on average for every 10 packets. Table 4 shows that the total reselection ratio is higher than 0.1 for all strategies to select the RRI when messages are aperiodic. This shows that LTE-V2X experiences additional reselections when handling aperiodic messages of variable size. These additional reselections actually prevent the depletion of *Reselection Counter*, and new resources are selected before *Reselection Counter* reaches zero. This is why the counter reselection ratio is smaller than 0.1 for all strategies to select the RRI. These strategies have an impact on the size and latency reselection ratios. If the RRI is set equal to 100 ms (strategy 1), the latency reselection ratio is close to zero[8] since 100 ms is the minimum time between CAMs in the *Empirical CAM model* and the risk to overpass the latency deadline is minimum. The latency reselection ratio increases with the second and third strategies. For example, sub-channels are reselected due to the latency deadline for 16.9% of the messages generated when the RRI is set equal to 200 ms (strategy 2). This number increases for the third strategy since the RRI can take values higher than 200 ms. Reselections due to changes in the size of messages are present with the three strategies to select the RRI. Table 4 shows that the size reselection ratio increases with the latency reselection ratio. When there is a reselection due to the latency deadline, it is possible that the new message or CAM has a small size. If this is the case, it is probable that the reserved sub-channels are not sufficient to transmit following messages of larger size. If this is the case, additional reselections would be needed. If there are no latency reselections (strategy 1), the selected sub-channels would be maintained for longer periods of time if the reselection is done for a message of large size; in this case, the selected sub-channels can be maintained until

[7] The ratios are independent of the traffic density since they are computed considering the messages generated per vehicle.

[8] The ratio is not equal to zero due to the jitter.

Reselection Counter reaches zero. The obtained results show that the strategy to select the RRI has a direct impact on the latency and size reselection ratios.

Table 5 reports the ratio of unused sub-channels and unutilized reservations for the three strategies to select the RRI. Table 4 and Table 5 show that the ratio of unused sub-channels is inversely related with the number of reselections. The selected sub-channels can be maintained until *Reselection Counter* reaches zero if the following messages fit in the selected sub-channels until *Reselection Counter* is depleted. This is more probable if the sub-channels were originally selected for a message of large size. If this is the case, it is actually probable that more sub-channels are reserved for the transmission of the following messages (or CAMs in our study) than actually needed for most of these messages (until *Reselection Counter* reaches zero). As a result, there is a higher probability to increase the number of sub-channels that are reserved but not used when the selected sub-channels are maintained for longer. On the other hand, a high number of reselections (e.g. due to the latency deadline) reduces the possibility to maintain the selected sub-channels until *Reselection Counter* reaches zero and therefore decreases the ratio of unused sub-channels. This explains the trends observed in Table 5 for the different strategies to select the RRI. The first strategy (i.e. RRI = 100 ms) reduces the ratio of reselections but increases the ratio of unused sub-channels. The second and third strategies increase the number of reselections but reduce the ratio of unused sub-channels. This is because more frequent reselections allow better adjusting the selected sub-channels to the actual size of the different messages. We should remember that unutilized reservations could result in packet collisions since other vehicles have fewer sub-channels available to reserve, and hence there is a higher risk that two vehicles reserve the same sub-channels. This risk is small when the channel load is small since there is a large number of available sub-channels. However, it increases with the channel load. This explains why the first strategy performs better than the other two strategies when the traffic density (and channel load) is low, but it performs worse when the traffic density increases (Fig. 17). The first strategy reduces the total reselection ratio but increases the number of unused sub-channels. A lower reselection ratio is positive for LTE-V2X and the negative effects of a large number of unused sub-channels appear under high traffic densities and channel loads.

TABLE 5. Unused Sub-channels and unutilized reservations (Empirical CAM model).

RRI strategy	Rate of unused sub-channels	Rate of unutilized reservations
1	0.225	0.815
2	0.18	0.367
3	0.143	0.118

Table 5 shows that the ratio of unutilized reservations is higher when the RRI is low. In particular, the first strategy results in a very high number of reservations that are never utilized. If a vehicle makes a reservation and does not transmit a TB in this reservation, it will not be able to announce its following transmissions. The other vehicles will then believe that the corresponding sub-channels will be free, and the risk of packet collisions increases for the following transmissions. The first strategy to select the RRI is the one that is more exposed to this risk since it results in many reservations (81.59% of all the reservations made) that are never utilized to transmit a TB or message. The first strategy therefore increases the ratio of unused sub-channels and unutilized reservations (Table 5). We should note that the negative effect of unused sub-channels or unutilized reservations increases with the traffic density and channel load since there is more demand for resources and the risk of packet collisions increases. This explains why the first strategy to select the RRI performs better with respect to the other strategies under low densities than under higher ones (Fig. 17). The first strategy increases the ratio of unused sub-channels and unutilized reservations. However, it also decreases the ratio of reselections (Table 4) and therefore reduces the risk of packet collisions due to frequent reselections. Opposite trends are observed for the other strategies with different values for the metrics depending on the selection of the RRI. This explains why the three strategies result in similar PDR levels (Fig. 17) with some differences depending on the traffic density and channel load. It also explains why none of the evaluated strategies can actually solve the challenges of LTE-V2X explained in Section III. Each strategy tends to reduce or mitigate one of the challenges but this is generally achieved at the expense of degrading the others. Fig. 19 provides a more graphical view of the differences between strategies to select the RRI. Fig. 19 clearly shows that none of the three strategies can actually minimize all challenges present in the sensing-based SPS scheme of LTE-V2X under the presence of aperiodic messages of variable size. For example, the first strategy minimizes the ratio of reselections but it maximizes the ratio of unutilized reservations. The contrary effect is observed with the third strategy. In the remaining sections, results for LTE-V2X will be shown with the best strategy to select the RRI in each scenario although there are no significant differences between strategies.

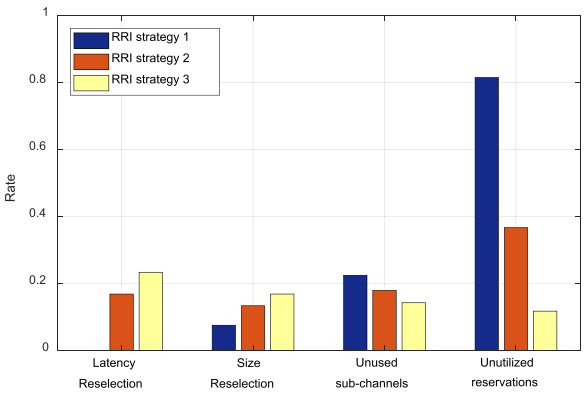

FIGURE 19. Impact of the strategies to select the RRI in LTE-V2X.

Finally, we would like to note that all the challenges quantified in this section are not present when considering periodic messages of constant size (i.e. *Simplified model*). In this case, only the counter reselection ratio (and the total reselection ratio) is equal to 0.1 since *Reselection Counter* is uniformly distributed between 5 and 15 and there would then be a reselection on average for every 10 packets. All other ratios shown in Table 4 and Table 5 are equal to zero. The challenges discussed in this section emerge as we introduce variability in the message generation.

D. MESSAGE SIZE VS TIME BETWEEN MESSAGES

The previous sections have shown that variations in size and time between messages (characteristic of the ETSI CAM messages) significantly degrade the performance of LTE-V2X mode 4 compared to IEEE 802.11p when the traffic density or channel load increases. This section analyzes the impact of variations of size and time between messages separately. To this aim, we utilize the *Empirical-size* and *Empirical-time* models described in Section IV.D. These models fix the size of messages or the time between messages, and model the other variable following the empirical traces. Fig. 20 depicts the PDR achieved with LTE-V2X mode 4 and IEEE 802.11p under medium CBR levels.[9] Fig. 20.a represents the PDR when the time between CAMs is fixed at 200 ms (the RRI is set equal to 200 ms) and the size of CAM varies. Fig. 20.b represents the PDR when the size of CAMs is fixed at 200 bytes and the time between CAMs varies (results are shown for the first strategy to select the RRI). Fig. 20 clearly shows that both variations in size or time between CAMs have a negative effect on the performance of LTE-V2X mode 4. We should note that Fig. 20.a has been obtained with a larger CBR than Fig. 20.b. In this case, and considering the trends observed in both figures, it is possible to conclude that variations in the time between messages or CAMs have a higher negative impact on the performance of LTE-V2X than variations in the size of CAMs. However, variations in the size of messages have also a relevant impact on LTE-V2X.

[9]Each model generates messages differently and the same traffic density results in different CBR levels. We then have to consider different traffic densities to achieve medium CBR levels with both models.

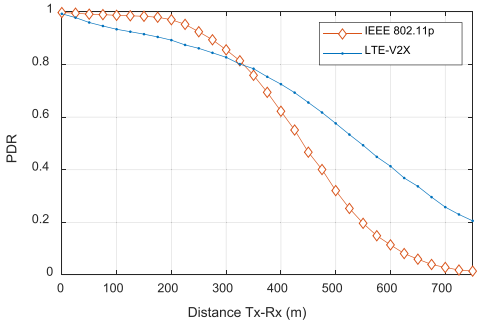

(a) *Empirical-size model*. 120 veh/km (CBR~0.33)

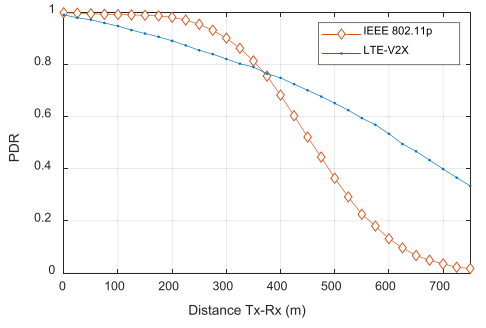

(b) *Empirical-time model*. 200 veh/km (CBR~0.23)

FIGURE 20. PDR experienced when CAM messages are generated following the *empirical separate models*.

E. OTHER CONFIGURATIONS

The previous evaluations have shown that different strategies to select the RRI cannot solve the challenges experienced by the LTE-V2X sensing-based SPS scheme when handling aperiodic messages of variable size. We now analyze the possibility to mitigate these challenges with the probability P to maintain the same sub-channel(s) when the *Reselection Counter* is depleted or with packet retransmissions. The previous evaluations have been conducted with $P = 0$ following the findings in [20]. Fig. 21 compares the PDR experienced with aperiodic messages of variable size (*Empirical CAM model*) when P is set equal to 0 and 0.8. LTE-V2X is configured with the first strategy to select the RRI and the RRI is set equal to 100 ms. This is the strategy that will mostly benefit from increasing P since it has the highest counter reselection ratio and the lowest size and latency reselection ratios (Table 4). Fig. 21 shows that IEEE 802.11p outperforms LTE-V2X when handling aperiodic messages of variable size independently of the value of P. Increasing P should reduce the probability to select different sub-channels when *Reselection Counter* is equal to 0 and therefore the total number of reselections. This is actually the case since increasing P from 0 to 0.8 reduces the total reselection ratio from 0.155 to 0.04 under the evaluated conditions. Reducing the number of reselections should improve the PDR. However, Fig. 21 shows that the improvement is small. This is because

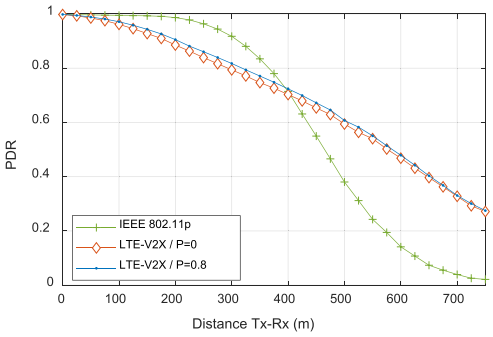

FIGURE 21. Impact of P on the PDR with aperiodic messages of variable size (*empirical CAM model*). Results are shown for a traffic density of 120 veh/km. Similar trends have been observed for other traffic densities.

reducing reselections by increasing P augments some of the other inefficiencies observed in LTE-V2X when transmitting aperiodic messages of variable size. In particular, increasing P to 0.8 augments the ratio of unused sub-channels from 0.225 to 0.282 and the ratio of unutilized reservations from 0.815 to 0.927. Augmenting these ratios reduces the capacity and increases the risk of packet collisions which ultimately impacts the PDR. This explains why there is no significant gain in PDR in Fig. 21 when increasing P from 0 to 0.8.[10]

The small improvement in PDR observed in Fig. 21 with $P = 0.8$ is obtained at the expense of increasing the probability of persistent packet collisions between two vehicles. If two vehicles select the same sub-channel(s) at a given moment, the probability that their packet collisions will persist over time increases with P. This is because higher values of P decrease the probability to select new sub-channel(s) when *Reselection Counter* reaches 0, and therefore also decrease the probability to break persistent packet collisions between vehicles. This is visible in Fig. 22 that plots the PIR (Packet Inter-Reception time) when LTE-V2X utilizes the first strategy to select the RRI. The figure shows that $P = 0.8$ increases the probability of experiencing a PIR of several seconds. A value of P equal to 0 is recommended in this case since the PDR is not highly improved when P is increased to 0.8, and persistent packet collisions can represent a significant safety risk. Fig. 22 also shows that IEEE 802.11p is less prone to persistent packet collisions than LTE-V2X.

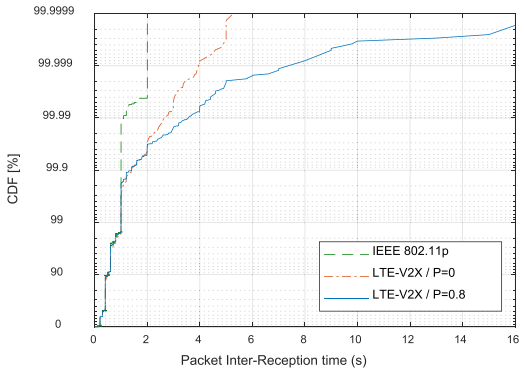

FIGURE 22. Impact of P on the PIR with aperiodic messages of variable size (*empirical CAM model*). Results are shown for a traffic density of 120 veh/km. Similar trends have been observed for other traffic densities.

The impact of P on LTE-V2X mode 4 when transmitting periodic messages was evaluated by the authors in [20]. This study considered both the *Simplified model* and the *3GPP model*. The study showed that augmenting P can slightly improve the PDR with periodic messages of constant size because vehicles tend to maintain the same sub-channels when *Reselection Counter* is depleted. This benefit was particular noticeable under low channel loads. However, the study also showed that augmenting P can degrade the PDR when the channel load increases and LTE-V2X transmits periodic messages of constant size (*Simplified model*). The positive impact of augmenting P was more visible (although the improvement in PDR was not very high) when the periodic messages have different sizes (i.e. with the *3GPP model*). This was the case because the reduction of reselections caused by augmenting P compensated the additional reselections resulting from variations in the size of messages. Readers are referred to [20] for a complete analysis of the impact of P when transmitting periodic messages (including numerical results of the discussed trends).

LTE-V2X offers the possibility to transmit each packet twice to increase the reliability of sidelink V2X communications. Authors demonstrated in [10] that retransmissions can have a positive impact under low traffic densities. However, the impact of retransmissions is negative when the channel load increases since retransmissions augment the probability of packet collisions. The analysis in [10] was conducted considering periodic messages. In our implementation, receiving vehicles do not use chase combining and each copy of a packet is decoded independently. The packet is received correctly if at least one of the two copies is correctly received. Fig. 23 shows that retransmissions actually degrade the performance of LTE-V2X mode 4 (configured with the RRI equal to 100 ms) even under low traffic densities when transmitting aperiodic messages of variable size (*Empirical CAM model*). Retransmissions increase the channel load[11] and the load amplifies the challenges of the sensing-based SPS scheme under the presence of aperiodic messages of variable size (Section III). This is why the PDR is degraded in Fig. 23 when retransmissions are allowed. These results limit the benefit of retransmissions to weak links under very low channel load levels.

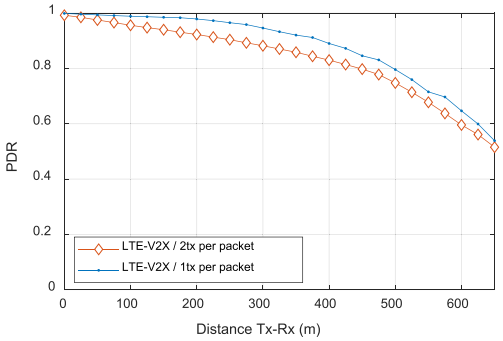

FIGURE 23. Impact of retransmissions in LTE-V2X. Traffic density of 60 veh/km.

The results shown so far have been obtained with the sensitivity levels reported for commercial devices or prototypes (−92 dBm for IEEE 802.11p and −103.5 dBm for LTE-V2X). These sensitivity levels are higher than the minimum sensitivity levels specified in IEEE 802.11p (−85 dBm)

[10]The second and third strategies to select the RRI result in more latency and size reselections than the first strategy (Table 4). These additional reselections result in that vehicles will have to select more frequently new sub-channels before the *Reselection Counter* is depleted. In this case, increasing P would have a smaller impact on the second and third strategies.

[11]Retransmissions increase the CBR from 0.095 to 0.187 when the traffic density is 60 veh/km and we use the *Empirical CAM model*.

and LTE-V2X (−90.4 dBm) standards. We now analyze the performance when considering these minimum sensitivity levels. Fig. 24 shows the PDR achieved when both standards operate with their minimum sensitivity levels and they transmit aperiodic messages of variable size (*Empirical CAM Model*). LTE-V2X is configured with the first strategy to select the RRI that is set equal to 100 ms. It should be noted that LTE-V2X has a better minimum sensitivity level than IEEE 802.11p. Reducing the sensitivity level reduces the communication range and hence decreases the CBR. A lower CBR benefits LTE-V2X since it reduces the impact of the challenges present in the sensing-based SPS of LTE-V2X when transmitting aperiodic messages of variable size (Section III). This explains why LTE-V2X improves its performance at short and medium distances compared to IEEE 802.11p in Fig. 24. However, the same trends previously described with aperiodic messages are observed in Fig. 24 when comparing LTE-V2X and IEEE 802.11p at medium and high distances.

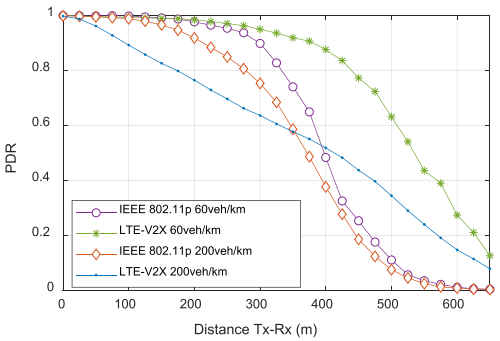

FIGURE 24. PDR using minimum sensitivity levels for both standards. Results are shown for 60 veh/km and 200 veh/km when transmitting aperiodic messages of variable size (*empirical CAM model*).

The analysis of the empirical CAM traces reported in [14] showed that CAMs were not always generated in multiples of 100 ms and that there is in fact some jitter. This jitter is included in the *Empirical CAM model* as described in Section IV.C. We have analyzed whether the jitter produces additional reselections due to the latency deadline. Our analysis has shown that the impact of the jitter on the performance of LTE-V2X mode 4 is negligible and the same PDR is achieved whether the jitter is included or not in the generation of CAM messages. This is because the jitter is small (its standard deviation is around 3 ms) and nearly does not have an impact on the latency reselection ratio.

F. SAME PHYSICAL LAYER FOR IEEE 802.11p AND LTE-V2X

The previous results have been obtained considering the physical layer performance reported in [3] as well as different sensitivity levels for both standards. All these configurations result in a worse link budget and physical layer for IEEE 802.11p compared to LTE-V2X. Certain studies claim that the physical layer of IEEE 802.11p can be improved with better receiver designs [31]. We then compare in Fig. 25 the performance of LTE-V2X and IEEE 802.11p when both

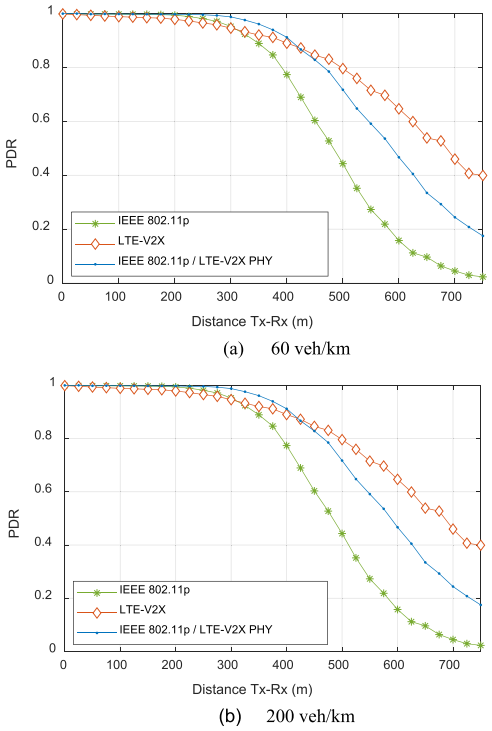

FIGURE 25. PDR when IEEE 802.11p is configured with the physical layer and sensitivity levels of LTE-V2X (802.11p/LTE-V2X PHY in the figure). Results are reported for aperiodic messages of variable size (*empirical CAM model*).

standards are configured with the same sensitivity levels and equal physical layer performance (using for both standards the BLER-SINR curves of LTE-V2X reported in [3]). This evaluation addresses a hypothetical scenario where IEEE 802.11p can overcome its lower physical layer performance compared to LTE-V2X. We should note that the results reported in Fig. 25 have been obtained considering a different thermal noise for both standards. This is the case because IEEE 802.11p utilizes the complete 10 MHz bandwidth for each transmission while LTE-V2X only utilizes a subset of RBs or sub-channels depending on the size of the messages. Fig. 25 plots the PDR when IEEE 802.11p is configured with its physical layer and sensitivity level (IEEE 802.11p in Fig. 25) and when it is configured with the physical layer and sensitivity levels of LTE-V2X (IEEE 802.11p/LTE-V2X PHY in Fig. 25). Fig. 25 compares the PDR with two traffic densities and considering aperiodic CAMs of variable size (*Empirical CAM model*). LTE-V2X is configured with the best strategy to select the RRI (first strategy in Fig. 25.a and second in Fig. 25.b). Fig. 25 shows that improving the physical layer and sensitivity levels of IEEE 802.11p improves the performance of IEEE 802.11p for all distances. This reduces the benefits of LTE-V2X under low traffic densities and augments the gains of IEEE 802.11p over LTE-V2X when the traffic density and channel load augment. We should also highlight that the capture effect results in that IEEE 802.11p can maintain or improve the PDR at short distances even if the communication range (and therefore the probability to interfere other vehicles) increases with a better physical

layer and sensitivity level. We can observe in Fig. 25.a that LTE-V2X improves the PDR at large distances compared to IEEE 802.11p even when IEEE 802.11p is evaluated with the same physical layer and sensitivity level than LTE-V2X. This is due to the impact of noise since LTE-V2X utilizes less bandwidth to transmit a message compared to IEEE 802.11p that utilizes the complete 10 MHz channel and is then more affected by noise.

VII. DISCUSSION

This study has shown that V2X technologies can see their performance degrade as the channel load increases. Such increase can be accelerated with the deployment of connected automated vehicles and the introduction of advanced V2X applications. Vehicular networks can use congestion control algorithms to control the channel load and ETSI has defined the Decentralized Congestion Control (DCC) framework for this purpose. However, we should note that congestion control has not been necessary in this study since the resources demanded by each vehicle in the simulated scenarios are below the limits imposed by DCC as we show next.

In LTE-V2X [36], each vehicle measures the CBR and adjusts its CR (channel occupancy ratio) to comply with the CR limit values provided in [36]. The CR is defined as the ratio of the total number of sub-channels used by a vehicle to the total number of sub-channels over a measurement period of 1000 ms [36]. The standard defines different CR limits based on priorities (PPPP, ProSe per-packet priority) so that critical messages can be prioritized in congested scenarios. According to [37], CAMs are classified as PPPP5. Table 6 shows there is no limit in the transmission of CAMs if the CBR is below 0.3. If the CBR is between 0.3 and 0.65, the CR limit is 0.03, i.e. a vehicle can use 3% of the sub-channels for transmitting its CAMs. If the CBR is between 0.65 and 0.8, the CR limit is 0.006, i.e. a vehicle can use 0.6% of the sub-channels for transmitting its CAMs. Our study considers 5 sub-channels per sub-frame following [38]. The maximum number of sub-channels that a vehicle can use in 1000 ms is then equal to the CR limit multiplied by 5000. This maximum number is also shown in Table 6. In this study, the number of sub-channels used by an LTE-V2X vehicle every 1000 ms is always below the maximum number as shown in Table 6. This means that congestion control is never activated and vehicles do not need to reduce their CR. To demonstrate it, we analyze the highest traffic density scenario (400 veh/km) with vehicles using the *Simplified model* or the *Empirical CAM model*. When vehicles generate CAMs following the *Simplified model*, the average CBR is equal to 0.638 and the CBR is always below 0.8 in the highest traffic density scenario. In this case, the most restrictive CR limit is 0.006, which means that each vehicle can use at most 30 sub-channels every 1000 ms (Table 6). The *Simplified model* generates CAMs of 200 bytes every 200 ms. Each CAM needs 2 sub-channels with the considered MCS, and therefore a vehicle needs 10 sub-channels every 1000 ms to transmit all its CAMs. This number is quite below the limit of 30 sub-channels imposed when the CBR is between 0.65 and 0.8. The CR is then always below the CR limit and congestion control is not activated. When vehicles generate CAMs following the *Empirical CAM model*, the CBR measured is always below 0.65. The CR limit is equal to 0.03 when the CBR is in the range 0.3-0.65. This means that each vehicle can use up to 150 sub-channels every 1000 ms. The *Empirical CAM model* generates variable CAMs so the number of sub-channels needed by a vehicle every 1000 ms varies. In our study, a vehicle can transmit a maximum of 10 packets per second and a CAM occupies at most 4 sub-channels. A vehicle then requires at most 40 sub-channels every 1000 ms to transmit all its CAMs. Since the limit is 150 sub-channels, we are again far below the CR limit even for the worst-case scenario. Congestion control is then not activated since the resources demanded by each vehicle are below the limits established by congestion control.

TABLE 6. CR limits defined in [36] and corresponding maximum number of sub-channels that an LTE-V2X vehicle can use every 1000 ms for PPPP3 and PPPP5.

CBR measured	CR limit	Max. sub-channels
$0 \leq \text{CBR} \leq 0.3$	No limit	No limit
$0.3 < \text{CBR} \leq 0.65$	0.03	150
$0.65 < \text{CBR} \leq 0.8$	0.006	30
$0.8 < \text{CBR} \leq 1$	0.003	15

The congestion control limits for IEEE 802.11p are defined in [39] and [40]. These specifications establish that, independently of the channel load, the packet transmission duration (T_{on}) and that the duty cycle must be always below 4 ms and 3% respectively. The duty cycle is defined as the ratio of the transmitter total ''on'' time relative to 1 second period. We consider again the highest traffic density and the *Simplified* and *Empirical CAM* models. In all cases, vehicles transmit with a 6 Mbps data rate. When vehicles generate CAMs using the *Simplified model*, T_{on} is equal to 0.36 ms and the duty cycle is equal to 0.18%. The congestion control requirements are therefore satisfied and congestion control is not activated. We have also measured T_{on} and the duty cycle when vehicles generate CAMs following the *Empirical CAM model*. T_{on} and duty cycle are always below 4 ms and 3% respectively. The maximum values measured for Ton and duty cycle are 0.7 ms and 0.8% respectively. Again, these values are far below the limits established in [39] and [40]. ETSI specifications define additional limits that depend on the CBR. For CBR$<$0.62, the time interval between messages (T_{off}) must be higher than 25 ms, i.e. the message transmission rate must be lower than 40 Hz. For CBR$\geq$0.62, the following equation must be satisfied:

$$T_{off} \geq \min\left\{1000\text{ ms}, T_{on} \times \left(4000 \times \frac{CBR - 0.62}{CBR} - 1\right)\right\} \quad (1)$$

In our study, the maximum CAM transmission rate is 10 Hz. In this case, the $T_{off} > 25$ ms condition for

CBR<0.62 is always satisfied. CBR values higher than 0.62 were only experienced in the highest traffic density scenario (400 veh/km). Fig. 26 shows the PDF of the CBR experienced when vehicles generate CAMs with the *Simplified* or *Empirical CAM* models in the scenario with 400 veh/km. The figure shows that the CBR is always below 0.68 when vehicles use the *Simplified model* and below 0.66 when they use the *Empirical CAM model* to generate CAMs. If we use the *Simplified model* with $T_{on} = 0.36$ ms and CBR = 0.68 (highest CBR in Fig. 26), equation (1) indicates that $T_{off} \geq 126,7$ ms. Since the *Simplified model* generates CAMs every 200 ms, the congestion control requirements specified in [39] and [40] are always satisfied for IEEE 802.11p in our study. The *Empirical CAM model* generates CAMs with variable size and time between CAMs. Under the highest traffic density, the percentage of CAMs that satisfy equation (1) – and hence the congestion control requirements – is 100% for CBR values below 0.65. This percentage is equal to approximately 99% and 97% when the CBR is equal to 0.65 and 0.66 respectively. We can derive the probability of experiencing a CBR of 0.65 and 0.66 from Fig. 26. Using this information, the probability that a CAM generated with the *Empirical CAM model* does not satisfy equation (1) is approximately 0.0003. This means that if congestion control was enabled, it would only affect 0.03% of the CAM messages generated with the *Empirical CAM model* in the highest traffic density scenario (400 veh/km). Congestion control will not affect the rest of CAM messages in this scenario or any of the CAM messages generated in the scenarios with lower traffic densities. This analysis and discussion explains why congestion control would not impact the results presented in this study. However, this impact should be taken into account if considering scenarios that surpass the congestion control limits due to higher channel load levels and/or higher channel occupancy per vehicle.

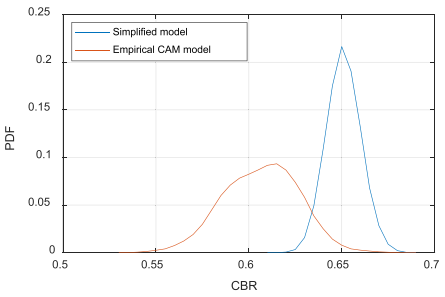

FIGURE 26. PDF of the CBR measured for 400 veh/km with IEEE 802.11p.

The channel load and channel occupancy can be reduced using MCS with high data rates. This study has though been conducted using a fixed MCS for LTE-V2X and IEEE 802.11p with approximately equal data rates. It is left for future study the possibility to improve the operation and performance of LTE-V2X and IEEE 802.11p through a dynamic selection of the MCS. Selecting a high MCS can reduce the channel occupancy and hence the probability of packet collisions. However, this is done at the expense of a lower error protection against transmission errors. There are then trade-offs that must be carefully studied. The authors already showed in [4] that the use of high MCSs (i.e. MCSs offering high data rates) can reduce the channel load in IEEE 802.11p. In LTE-V2X, we could also use high MCSs to transmit large messages in the same number of sub-channels as smaller ones. This would reduce the number of reselections due to variations in the message size and hence improve the operation of the sensing-based SPS scheme. Adapting the MCS to the message and sub-channel size is straightforward when considering a limited number of message sizes (e.g. in the *3GPP model*). However, current and future vehicular standards will generate messages of variable size. In this context, optimizing the selection of MCSs in LTE-V2X is not a trivial task and it is an in-depth analysis that has not been conducted to date and that is beyond the scope of this paper. There are several trade-offs and effects that should be carefully considered in this analysis. A high MCS can reduce the number of RBs needed to transmit a message. However, increasing the MCS might not reduce the number of sub-channels needed to transmit a message as illustrated in Fig. 27. The capacity to reduce the number of sub-channels to transmit a message depends on the message size, the available MCS and the size of sub-channels. Defining an effective strategy to vary the MCS so that messages of different sizes can fit in the same number of sub-channels requires first a careful study to optimize the LTE-V2X sub-channelization (i.e. the size of sub-channels and the number of sub-channels per sub-frame) based on the available MCSs and the possible message sizes. This study should take into account that the sub-channelization cannot be dynamically modified and it should adequately serve all vehicles and possible operating conditions (e.g. channel load). Vehicles can modify their MCS based on these conditions but they cannot dynamically change the sub-channelization and the sub-channelization must be the same for all vehicles in a scenario. Once the sub-channelization is configured, it is also necessary to analyze if using higher MCS to transmit messages of larger size really improves the operation of LTE-V2X. Modifying the MCS could help transmit messages of different size in the same number of sub-channels. This would improve the operation of the sensing-based SPS scheme by avoiding reselections due to changes in the message size. However, this

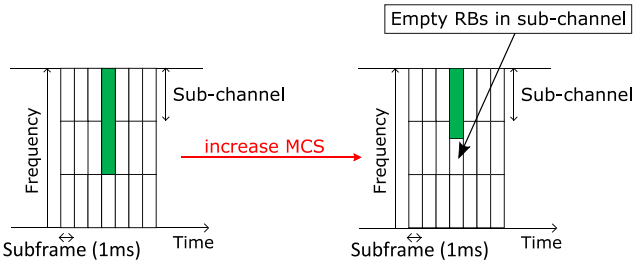

FIGURE 27. Illustration of a scenario where augmenting the MCS does not reduce the number of sub-channels with a given LTE-V2X sub-channelization.

might not be straightforward if messages can have multiple sizes as it is the case of CAMs; even more variable message sizes can be expected for example for cooperative perception if we take into account the current ETSI proposal for the CPM (Collective Perception Message) format [41]. In addition, if all messages have to fit in the same number of sub-channels, high MCSs would only be utilized to transmit messages of large size. This would prevent using high MCSs to transmit messages with smaller size which can have a negative impact on the possibility to control congestion levels if we take into account that, for example, the majority of CAMs have a small size. This discussion highlights that defining the best strategy to vary the MCS as a function of the message size is not trivial in LTE-V2X and requires a careful study that should include an analysis of the most adequate configuration of the LTE-V2X sub-channelization and the possibility to transmit messages of multiple sizes. This study has not been conducted to date and is beyond the scope of this paper. In addition, and following the findings in [4], we should also take into account that IEEE 802.11p could also improve its performance through a dynamic selection of the MCS.

VIII. CONCLUSIONS

This paper has presented an in-depth system level comparison of the performance of IEEE 802.11p and LTE-V2X when transmitting periodic and aperiodic messages with constant or variable size. The comparison has been conducted with different message generation models so that it is possible to analyze the impact of the time between messages and their size. This has included simple models that generate periodic messages of constant size but also a realistic model that generates messages following the ETSI CAM standard. This model was developed using field traces collected by OEMs that implemented the ETSI standard. The conducted analysis has demonstrated that LTE-V2X can achieve better performance than IEEE 802.11p under low channel loads if it has a better physical layer performance. Under low channel load levels, the MAC has a lower impact on the performance than the physical layer. However, IEEE 802.11p outperforms LTE-V2X when the channel load increases even if it has a lower physical layer performance. The gains obtained with IEEE 802.11p are present even with periodic messages of constant size but they significantly augment when messages are aperiodic and vary their size. This is the case because the sensing-based SPS scheme included in LTE-V2X experiences important challenges when handling aperiodic messages and messages of variable sizes. These challenges have been demonstrated and quantified in this study for the first time. The study has also shown that these challenges cannot be completely overcome with certain configurations of LTE-V2X (as currently defined by the 3GPP standard) since each configuration analyzed mitigates one challenge but aggravates others. We would like to highlight that this study has been conducted considering the ETSI CAM standard that is being deployed in Europe (and maybe other regions of the world). Other regions might implement other standards for the generation of the basic awareness messages, and each standard may generate messages with different patterns (in terms of size and time between messages). It would be interesting that other studies replicate this analysis considering these standards if realistic message generation models would be available. However, we would like to note that the challenges described for the LTE-V2X MAC exist by design of the standard and their impact will depend on the characteristics of the messages to be transmitted. Such dependency is less present in IEEE 802.11p that includes a simpler but more flexible MAC. We would also like to highlight that this study has been conducted considering different message generation models that go from completely periodic messages of constant size (which is the best possible scenario for LTE-V2X) to aperiodic messages of variable size following the ETSI CAM standard. Other message generation standards (e.g. BSM) will create message patterns different from CAM but these patterns will be bounded by the periodic and constant size scenario considered in this study and the aperiodic and variable size one represented by the ETSI CAM standard.

REFERENCES

[1] A. Filippi, K. Moerman, V. Martinez, and A. Turley, "IEEE802.11p ahead of LTE-V2V for safety applications," NXP Semicond., Eindhoven, The Netherlands, Autotalks, Kfar Netter, Israel, White Paper, Sep. 2017. [Online]. Available: https://www.nxp.com/docs/en/white-paper/LTE-V2V-WP.pdf

[2] 5G Automotive Association, "An assessment of LTE-V2X (PC5) and 802.11p direct communications technologies for improved road safety in the EU," 5G Automot. Assoc., Munich, Germany, 5GAA White Paper, Dec. 2017. [Online]. Available: https://5gaa.org/wp-content/uploads/2017/12/5GAA-Road-safety-FINAL2017-12-05.pdf

[3] J. Hu, S. Chen, L. Zhao, Y. Li, J. Fang, B. Li, and Y. Shi, "Link level performance comparison between LTE V2X and DSRC," *J. Commun. Inf. Netw.*, vol. 2, no. 2, pp. 101–112, Jun. 2017.

[4] M. Sepulcre, J. Gozalvez, and B. Coll-Perales, "Why 6 Mbps is not (always) the optimum data rate for beaconing in vehicular networks," *IEEE Trans. Mobile Comput.*, vol. 16, no. 12, pp. 3568–3579, Dec. 2017.

[5] R. Molina-Masegosa and J. Gozalvez, "System level evaluation of LTE-V2V mode 4 communications and its distributed scheduling," in *Proc. IEEE 85th Veh. Technol. Conf. (VTC Spring)*, Jun. 2017, pp. 1–5.

[6] L. Zhao, J. Fang, J. Hu, Y. Li, L. Lin, Y. Shi, and C. Li, "The performance comparison of LTE-V2X and IEEE 802.11p," in *Proc. IEEE Vehicular Technol. Conf. (VTC-Spring)*, Porto, Portugal, Jun. 2018, pp. 1–5.

[7] M. Wang, M. Winbjork, Z. Zhang, R. Blasco, H. Do, S. Sorrentino, M. Belleschi, and Y. Zang, "Comparison of LTE and DSRC-based connectivity for intelligent transportation systems," in *Proc. IEEE 85th Veh. Technol. Conf. (VTC Spring)*, Sydney, NSW, Australia, Jun. 2017, pp. 1–5.

[8] T. V. Nguyen, P. Shailesh, B. Sudhir, G. Kapil, L. Jiang, Z. Wu, D. Malladi, and J. Li, "A comparison of cellular vehicle-to-everything and dedicated short range communication," in *Proc. IEEE Veh. Netw. Conf. (VNC)*, Turin, Italy, Nov. 2017, pp. 101–108.

[9] T. Shimizu, H. Lu, J. Kenney, and S. Nakamura, "Comparison of DSRC and LTE-V2X PC5 mode 4 performance in high vehicle density scenarios," in *Proc. ITS World Congr.*, Singapore, Oct. 2019, pp. 1–7.

[10] R. Molina-Masegosa and J. Gozalvez, "LTE-V for sidelink 5G V2X vehicular communications: A new 5G technology for short-range vehicle-to-everything communications," *IEEE Veh. Technol. Mag.*, vol. 12, no. 4, pp. 30–39, Dec. 2017.

[11] *Study on LTE-Based V2X Services (v14.0.0, Release 14)*, document TR 36.885, 3GPP, Jul. 2016.

[12] *Intelligent Transport Systems (ITS); Vehicular Communications; Basic Set of Applications; Part 2: Specification of Cooperative Awareness Basic Service*, document EN 302 637-2 V1.4.1, ETSI, Jan. 2019.

[13] *Dedicated Short Range Communications (DSRC) Message Set Dictionary*, document SAE J2735, SAE International, DSRC Technical Committee, Nov. 2009.
[14] *Survey on ITS-G5 CAM Statistics*, document TR2052, V1.0.1, CAR 2 CAR Communication Consortium, Dec. 2018.
[15] Q. Chen, F. Schmidt-Eisenlohr, D. Jiang, M. Torrent-Moreno, L. Delgrossi, and H. Hartenstein, "Overhaul of ieee 802.11 modeling and simulation in ns-2," in *Proc. 10th ACM Symp. Model., Anal., Simulation wireless mobile Syst. (MSWiM)*, Chania, Greece, 2007, pp. 159–168.
[16] 3GPP, "TS 36.213 Evolved Universal Terrestrial Radio Access (E-UTRA); Physical layer procedures (v14.12.0, Release 14)," 3GPP, Tech. Rep., Sep. 2019.
[17] *Evolved Universal Terrestrial Radio Access (E-UTRA); Radio Resource Control (RRC); Protocol specification (v14.12.0, Release 14)*, document TS 36.331, 3GPP, Sep. 2019.
[18] *Access Layer Specification for ITS Using LTE-V2X Communication in the 5,9 GHz Frequency Band*, document TS 103 613, V1.1.1, ETSI, Nov. 2018.
[19] *Evolved Universal Terrestrial Radio Access (E-UTRA); Medium Access Control (MAC) Protocol Specification (v14.11.0, Release 14)*, document TS 36.321, 3GPP, Jun. 2019.
[20] R. Molina-Masegosa, J. Gozalvez, and M. Sepulcre, "Configuration of the C-V2X mode 4 sidelink PC5 interface for vehicular communication," in *Proc. 14th Int. Conf. Mobile Ad-Hoc Sensor Netw. (MSN)*, Shenyang, China, Dec. 2018, pp. 43–48.
[21] M. Noor-A-Rahim, G. G. M. N. Ali, H. Nguyen, and Y. L. Guan, "Performance analysis of IEEE 802.11p safety message broadcast with and without relaying at road intersection," *IEEE Access*, vol. 6, pp. 23786–23799, 2018.
[22] A. Bazzi, G. Cecchini, A. Zanella and B. M. Masini, "Study of the impact of PHY and MAC parameters in 3GPP C-V2V mode 4," *IEEE Access*, vol. 6, pp. 71685–71698, 2018.
[23] A. Mansouri, V. Martinez, and J. Harri, "A first investigation of congestion control for LTE-V2X mode 4," in *Proc. 15th Annu. Conf. Wireless demand Netw. Syst. Services (WONS)*, Jan. 2019, pp. 56–63.
[24] A. Nabil, K. Kaur, C. Dietrich, and V. Marojevic, "Performance analysis of sensing-based semi-persistent scheduling in C-V2X networks," in *Proc. IEEE 88th Veh. Technol. Conf. (VTC-Fall)*, Chicago, IL, USA, Aug. 2018, pp. 1–5.
[25] A. Bazzi, A. Zanella, and B. M. Masini, "Optimizing the resource allocation of periodic messages with different sizes in LTE-V2V," *IEEE Access*, vol. 7, pp. 43820–43830, 2019.
[26] R. Molina-Masegosa, M. Sepulcre, J. Gozalvez, F. Berens, and V. Martinez, "Empirical models for the realistic generation of cooperative awareness messages in vehicular networks," *IEEE Trans. Veh. Technol.*, vol. 69, no. 5, pp. 5713–5717, May 2020.
[27] *E-UTRA and E-UTRAN; Overall Description; Stage 2 (v14.11.0, Release 14)*, document TS 36.300, 3GPP, Sep. 2019.
[28] M. Gonzalez-Martín, M. Sepulcre, R. Molina-Masegosa, and J. Gozalvez, "Analytical models of the performance of C-V2X mode 4 vehicular communications," *IEEE Trans. Veh. Technol.*, vol. 68, no. 2, pp. 1155–1166, Feb. 2019.
[29] *HCM 2010: Highway Capacity Manual, Transportation Research Board*, Nat. Res. Council, Washington, DC, USA, 2010.
[30] *Guidelines for Evaluation of Radio Interface Technologies for IMT-Advanced*, document Report ITU-R M.2135-1, Dec. 2019.
[31] A. Turley, K. Moerman, A. Filippi, and V. Martinez, "C-ITS: Three observations on LTE-V2X and ETSI ITS-G5. A comparison," NXP, Eindhoven, The Netherlands, White Paper CITSCOMPWP REV 0, 2018. [Online]. Available: https://www.nxp.com/docs/en/white-paper/CITSCOMPWP.pdf
[32] *E-UTRA; User Equipment (UE) Radio Transmission and Reception (v14.13.0, Release 14)*, document TS 36.101, 3GPP, Oct. 2019.
[33] *Part 11: Wireless LAN Medium Access Control (MAC) and Physical Layer (PHY) Specifications*, IEEE Standard 802.11-2012, IEEE Computer Society, LAN/MAN Standards Committee, Mar. 2012.
[34] 5GAA, "V2X functional and performance test report; test procedures and results," 5G Automot. Assoc., Munich, Germany, 5GAA White Paper P-190033, Apr. 2019. [Online]. Available: https://5gaa.org/wp-content/uploads/2018/11/5GAA_P-190033_V2X-Functional-and-Performance-Test-Report_final-1.pdf
[35] *Cohda Mobility MK5 Module Datasheet, V1.2.0*, Cohda Wireless, Wayville, SA, Australia, May 2015.
[36] *Intelligent Transport Systems (ITS); Congestion Control Mechanisms for C-V2X PC5 Interface; Access Layer Part*, document TS 103 574, V1.1.1, ETSI, Nov. 2018.
[37] *Intelligent Transport Systems (ITS); Access Layer Specification for Intelligent Transport Systems Using LTE Vehicle to Everything Communication in the 5,9 GHz Frequency Band*, document TS 103 613, V1.1.1, ETSI, Nov. 2018.
[38] *Intelligent Transport Systems (ITS); LTE-V2X Access Layer Specification for Intelligent Transport Systems Operating in the 5 GHz Frequency Band*, document EN 303 613, V1.1.1, ETSI, Nov. 2019.
[39] *Intelligent Transport Systems (ITS); Radiocommunications Equipment Operating in the 5855 MHz to 5925 MHz Frequency Band; Harmonised Standard Covering the Essential Requirements of Article 3.2 of Directive 2014/53/EU*, document EN 302 571, V2.1.1, ETSI, Feb. 2017.
[40] *Intelligent Transport Systems (ITS); Cross Layer DCC Management Entity for Operation in the ITS G5A and ITS G5B Medium*, document TS 103 175, V1.1.1, ETSI, Jun. 2015.
[41] *Intelligent Transport Systems (ITS); Vehicular Communications; Basic Set of Applications; Analysis of the Collective Perception Service (CPS)*, document TR 103 562, V2.1.1, ETSI, Dec. 2019.

RAFAEL MOLINA-MASEGOSA received the degree in telecommunications engineering from the University of Granada (UGR), Spain. He is currently pursuing the Ph.D. degree in C-V2X and 5G vehicular networks with the Universidad Miguel Hernández de Elche (UMH), Spain. During his studies, he worked on brain image processing at the Signal Processing and Biomedical Applications (SiPBA) Group, UGR. In December 2015, he joined the UWICORE Research Laboratory, UMH.

JAVIER GOZALVEZ (Senior Member, IEEE) received the degree in electronics engineering from the Engineering School ENSEIRB, Bordeaux, France, and the Ph.D. degree in mobile communications from the University of Strathclyde, Glasgow, U.K. Since October 2002, he has been with the Universidad Miguel Hernández de Elche (UMH), Spain, where he is currently a Full Professor and the Director of the UWICORE Research Laboratory. At the UWICORE, he leads research activities in the areas of vehicular networks, 5G and beyond networks, and industrial wireless networks. He has been an Elected Member of the Board of Governors of the IEEE Vehicular Technology Society (VTS), since 2011, and served as the President of the IEEE VTS, in 2016 and 2017. He was an IEEE Distinguished Lecturer of the IEEE VTS and served as an IEEE Distinguished Speaker. He was the General Co-Chair of the IEEE VTC-Spring Conference, in 2015, and the General Co-Chair and the Founder of the IEEE Connected and Automated Vehicles Symposium, in 2018 and 2019. He is the Editor-in-Chief of the *IEEE Vehicular Technology Magazine*.

MIGUEL SEPULCRE (Senior Member, IEEE) received the degree in telecommunications engineering and the Ph.D. degree in communications technologies from the Universidad Miguel Hernández de Elche (UMH), Spain, in 2004 and 2010, respectively. He is currently an Associate a Professor with the Department of Communications Engineering, UMH, and a member of the UWICORE Research Laboratory, working in wireless vehicular networks. He has been a Visiting Researcher with ESA, Noordwijk, The Netherlands, in 2004, the Karlsruhe Institute of Technology, Germany, in 2009, and Toyota InfoTechnology Center, Tokyo, Japan, in 2014. He was awarded by the COIT (Spanish official association of telecommunication engineers) with the ONO Prize for the Best Ph.D. Thesis. He was the TPC Co-Chair of the IEEE VNC, in 2016, the IEEE VTC-Fall, in 2018, and the IEEE/IFIP WONS, in 2018. He serves as an Associate Editor for the *IEEE Vehicular Technology Magazine* and the IEEE COMMUNICATIONS LETTERS.